

April 2012

# Lizard Inspired Tail for Dynamic Stabilization of Robotic Body

Michael Christopher Berlied  
*Worcester Polytechnic Institute*

Follow this and additional works at: <https://digitalcommons.wpi.edu/mqp-all>

---

## Repository Citation

Berlied, M. C. (2012). *Lizard Inspired Tail for Dynamic Stabilization of Robotic Body*. Retrieved from <https://digitalcommons.wpi.edu/mqp-all/2927>

This Unrestricted is brought to you for free and open access by the Major Qualifying Projects at Digital WPI. It has been accepted for inclusion in Major Qualifying Projects (All Years) by an authorized administrator of Digital WPI. For more information, please contact [digitalwpi@wpi.edu](mailto:digitalwpi@wpi.edu).

# Lizard Inspired Tail for the Dynamic Stabilization of Robotic Bodies

---

A Major Qualify Project Report  
Submitted to the Faculty of  
WORCESTER POLYTECHNIC INSTITUTE  
in partial fulfillment of the requirements for the  
Degree of Bachelor of Science  
In Mechanical Engineering  
By

Michael Berlied \_\_\_\_\_

Approved by:  
Stephen Nestinger \_\_\_\_\_

Date Completed: April 27, 2012

## **ABSTRACT**

The purpose of this project was to determine the feasibility of a lizard inspired tail for the dynamic stabilization of robotic bodies during aerial or aggressive maneuvers. A mathematical model was created to determine the effects of various tail designs. A physical model of the tail design was fabricated and used to determine feasibility of the design and evaluate the mathematical model.

## Table of Contents

Abstract .....	ii
Table of Figures .....	v
1.0 Introduction.....	1
2.0 Methodology.....	2
3.0 Literature Review.....	3
3.1 Lizard Physiology and Tail Control.....	3
3.2 Tailbot Robotic Tail.....	6
3.4 Articulated Robotic Limbs.....	9
3.4.1 Festo Bionic Handling Assistant.....	10
3.6 Summary .....	12
4.0 Lizard Inspired articulated design synthesis .....	13
4.1 Assumptions and System Limitations.....	13
4.2 Control System for MDOF Manipulation.....	13
4.2.1 Serial Manipulator .....	14
4.2.2 Actuation Control.....	15
4.2.3 Implemented Design: Modified Actuation Control .....	15
4.3 Mass Distribution.....	16
4.4 Ligament Equivalent for Segment Connections .....	16
4.4.1 Tension Springs .....	18
4.4.2 Compression Springs .....	18
4.4.3 Flexible Rods .....	18
4.4.4 Implemented Ligament Connection.....	19
4.5 Segment Design .....	19
4.6 Summary .....	20
5.0 Modeling and Simulation.....	21
5.1 Vibration Analysis .....	21

5.1.1 Free Body Diagrams .....	22
5.1.2 Assumptions.....	23
5.1.3 Initial Value Problem.....	23
5.1.4 Operating Deflection Shapes and Modal Shapes.....	24
5.1.5 Vibrational Analysis Summary.....	30
5.2 MDOF Tail Modeling.....	30
5.2.1 Vector Rotation.....	31
6.0 Prototype Design.....	33
6.1 First Prototype.....	33
6.1.1 Design Review .....	34
6.1.2 Spring Location Iteration .....	34
6.2 Second Prototype .....	35
6.2.1 Design Review .....	35
7.0 Project Accomplishments and Discussions .....	38
8.0 Future Work .....	39
8.1 Physical Dynamics Model: Mathematical .....	39
8.2 Prototype Model.....	39
9.0 Conclusions.....	41
Bibliography .....	42
Appendix 1: MDOF Mathematical Modeling.....	43
Appendix 1.1: Modal Analysis Matlab Code .....	43
Appendix 1.2: Modal Flow Chart and Equation.....	46
Appendix 1.3: Vector Rotation Matlab Code .....	49
Appendix 2: Double Pendulum Modeling .....	52
Appendix 3: Quad Pendulum Modeling and Inertia Control.....	53

## TABLE OF FIGURES

Figure 1: Lizard Body Styles [7] .....	3
Figure 2: UC Berkeley Lizard Jumping Study [1].....	4
Figure 3: Sensitivity of Body Rotation to a Perturbation in a Lizard [1] .....	6
Figure 4: Robot Tail Effectiveness Testing and Correlation Data [1] .....	7
Figure 5: Tailbot nose-down perturbation based on tail manipulation. ....	7
Figure 6: Tail Effectiveness for Body Perturbations [1].....	8
Figure 7: Bio-mechatronic Robotic Examples of Festo [2] .....	10
Figure 8: Festo’s Bionic Handling Assistant [2] .....	11
Figure 9: Bionic Handling Assistant – Gripper [2].....	11
Figure 10: Serial Manipulator Example.....	14
Figure 11: Actuation Controlled Robot [3].....	15
Figure 12: Mass Distribution of Tail Design .....	16
Figure 13: Tension Spring Attachment Example.....	17
Figure 14: Quad Tension Spring Example.....	17
Figure 15: Compression Spring Example 1 .....	17
Figure 16: Compression Spring Example 2 .....	17
Figure 17: Mass Section Implemented Design .....	19
Figure 18: Free Body Diagrams and Equations for Modal Analysis .....	22
Figure 19: Lizard Tail Vibration Analysis.....	25
Figure 20: Second Vibrational Analysis (Opposite Lizard Tail) .....	27
Figure 21: Third Vibrational Analysis (Heavy M4) .....	29
Figure 22: Visual Example of Vector Rotation .....	31
Figure 23: Vector Rotation of Tail; Matlab Graphs.....	32
Figure 24: First Prototype .....	33
Figure 25: Prototype Two Manipulation Examples.....	35
Figure 26: Top and Back View of MDOF Movement.....	36
Figure 27: Modeling of Tail Stabilization Technique.....	37

## 1.0 INTRODUCTION

The basis for this project is that there is little to no research regarding dynamic stabilization of robotic bodies that constantly make aggressive or aerial maneuvers while traveling. If there is a robot that must be fast on a rough surface, like a survival robot, it is going to need constant stabilization to stay on track especially while being controlled remotely. While under operation, unwanted rotations and pitches from a rough surface can cause a robotic body to become unstable and potentially flip over causing it to become unusable. This project aims at solving this issue through the design of a controllable lizard inspired tail appendage.

Researchers at the University of California at Berkeley report that a lizard makes measured tail movements to stabilize itself when it is not balanced. This is called dynamic stabilization. Usually this occurs during sudden movements, especially through jumping and climbing where balance issues from gravitational forces are acting on the creature. They discovered that if its nose dives, it will thrust its tail upward, to offset the forward diving motion. This movement causes changes to its angular momentum, causing it to come upright once again. Many other animals have features like this that are not necessarily unique, but very functional. The simplicity and functionality of certain animal traits, like that of the lizard tail have recently been researched for new product design in robotics.

Using the research of the lizard tail, the UC Berkeley researchers designed a robot, Tailbot, which utilized this same functionality of the tail to keep a robot car upright through the air instead of allowing gravity to take its nose down through its forward momentum. Using gyroscopes and sensors, the tail would swing at a certain velocity to offset the unwanted motion of the robot through the air. However, they only did research on the vertical planar region for this experiment, essentially the tails ability to offset the forces of gravity only. Tailbot is unable to control body rotation or horizontal movements with the tail. The tail is only designed for one movement, at one instance through any aerial or aggressive maneuver [1].

The goal of this project is to design and model a lizard-inspired tail for use of dynamic stabilization control in aggressively moving robotic bodies. The most important aspect of the design is the capability to be maneuvered on all degrees of freedom. This will allow control of the roll, pitch, and yaw of a body as compared to only pitch control of Tailbot. A tail will be designed for continuous use capability as well as for the ability to control undesired rotations,

vertical movements, horizontal movements, and a combination of all of them at the same time. The use for this system would be for robots that make constant aggressive maneuvers such as a survival robot; fast moving robots that have to go quickly over rough, unknown terrain therefore needing constant stability.

## **2.0 METHODOLOGY**

There were two major goals of this project; design and build a prototype model of a lizard inspired tail that would be used for the dynamic stabilization of a robotic body as well the mathematical analysis of how effectively a tail of such design would manipulate an aggressively moving body. Background research was conducted first to determine if there was prior work pertaining to the project as well as gathering materials for use during the design process. Topics such as dynamic and kinematic modeling of multiple degree of freedom (MDOF) systems and robotic control systems for MDOF movement were researched.

The design process for the prototype model consisted of developing multiple design concepts, reviewing performance of each concept and then selecting and implementing the best design. This process was done for all aspects of the tail. Control systems, springs, materials, lengths, mass distribution, shape, etc. Each aspect was carefully considered, reviewed, and sometimes physically tested until a final design was reached. Final design was then tested as a whole to determine if it would meet the goals it was intended to. If it did not meet these goals, review of the failed concepts was conducted and an alternative design concept was implemented and then retested.

For the mathematical modeling of the tail, smaller, more realistic goals were set to provide a basis of direction toward the ultimately desired model. This combination of smaller works would be combined together to produce a larger model to meet the goal of the project. Each individual mathematical concept was researched independently from the others. Potential mathematical processes for each concept were researched. The process for each started with the simplest modeling. Once simple concepts were established, more variability was added to enhance the accuracy of the model. Testing and results of the model(s) were collected along the process; estimated/assumed input parameters were mostly used for the testing.



### 3.0 LITERATURE REVIEW

The following section provides the background information pertaining to the goals of this project as well as previous works that relate to the engineering aspects. A study regarding lizards and their ability to stabilize themselves during a jump is reviewed. Multiple degree of freedom robots already designed are reviewed for their control systems as design consideration for a tail. Understanding all the information about lizards, stabilization, and MDOF robotics there is critical to the design process.

#### 3.1 LIZARD PHYSIOLOGY AND TAIL CONTROL

In general, lizards are the most diverse group of all reptiles. Their sizes range from 0.8 inches up to 10 feet in length, which corresponds to 0.02 ounces to 330 pounds in weight range. There are some that use two feet to walk, others that use four and others that are limbless resembling snakes. Figure 1 shows an overview lizard species chart representative of the different body styles of lizards.

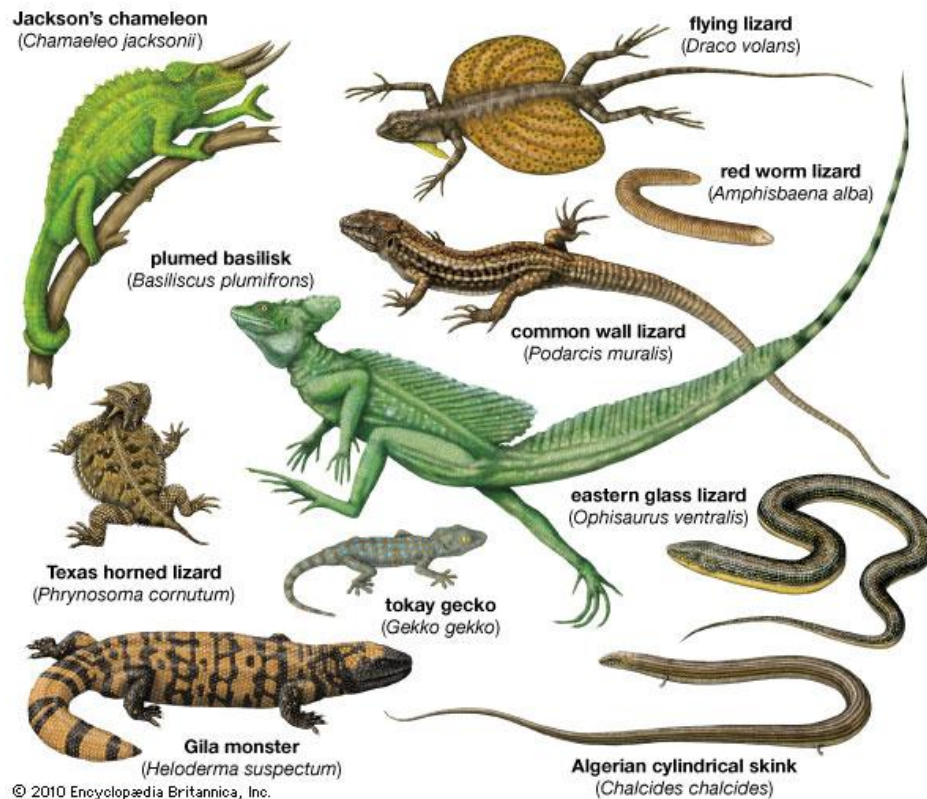
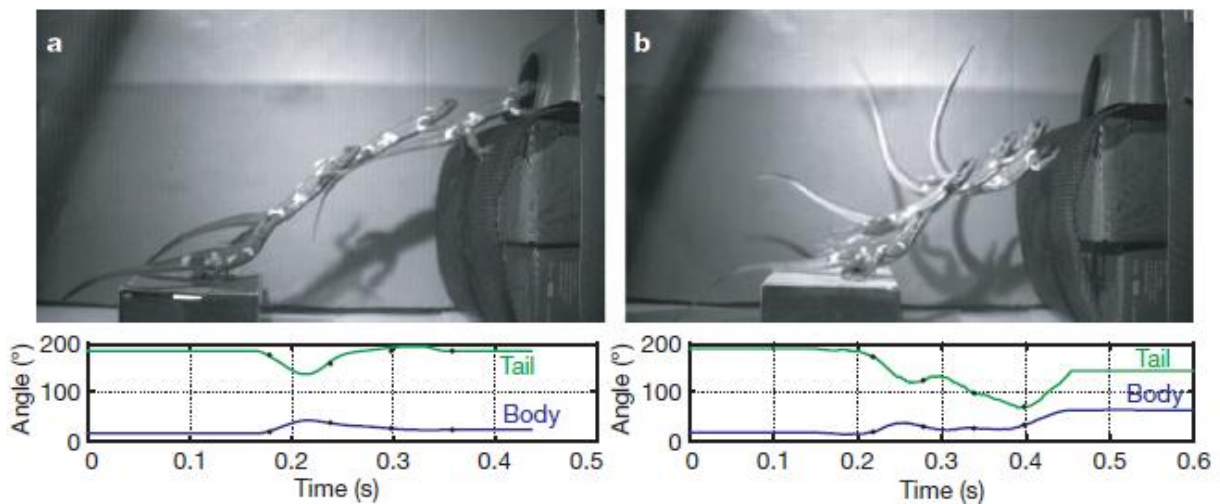


Figure 1: Lizard Body Styles [7]

With such diversity, each of these lizard species has a unique characteristic that defines its species. The flying lizard have wing like features that allow it to glide through the air while jumping, the plumed basilisk can walk/run on just its two hind legs in a motion known as locomotion. Using its tail to balance its weight until it is essentially weightless and its large hind legs in locomotion, a basilisk is able to not break the surface tension of water of a lake or pond; this allows it to run across water. This balancing act combined with the locomotion running style, could be used researched and tested in robotic applications in the future.

The popular conception of lizards is that of the common wall lizard averaging about 12 inches in length with a long, slender tail. Although this conception can only be applied to a small number of species in the lizard family, it was the size basis for the researchers at UC Berkeley when first examining the use of the tail in the balance of lizards in general. Specifically, they used red-headed agama lizards. They are considered unspecialized lizards that mostly dwell in rocky deserts and grow to be about 12-18 inches long [2].

Animal researchers at UC Berkeley conducted an experiment to understand the physiology of a lizard during a jump and the effect that the tail has for stabilization of the body. Two different surfaces were used to analyze controlled jump as compared to unexpected slippage during a jump. Figure 2 shows the results from this study.



**a) Lizard leap from friction surface**

**b) Lizard leap from slick surface**

**Figure 2: UC Berkeley Lizard Jumping Study [1]**

The first jump consisted of a lower platform covered with a high friction coating to allow lizard foot control to leap up to the higher platform. During the jump, the angle of the tail and

body were measured using a high speed camera and the data is seen below the picture. During this first jump, at 0.2 sec the lizard leaps up initiating a body movement; simultaneously, the lizard also lowers its tail below the horizontal. The correlation is that while the lizards body is moving 'up' the lizard moves its tail in the opposite direction to bring it back to the horizontal position, showing that the tail was used in stabilization of the body during this aerial maneuver.

For the second jump, part b, the launching platform was then covered in a low friction surface, not allowing the lizards feet to grab the surface and leap, but rather initiating a slip of the body. The measurements taken by the high speed camera show how important the tail use was for the stabilization of the body through the air in this maneuver. Because of the slip, the lizard was unable to initiate the body torque from its front legs like it did during first jump, and instead uses its tail to initiate this torque. Tail angle goes from 200 degrees to about 75 degrees in 0.2 seconds; this is almost triple the angle it used for the first jump. However, the body angle through the entire jump stays relatively normal despite the slip. This proves that a lizard uses its tail mass to initiate stabilization when undesired motions are happening; this phenomenon is the basis for this project [1].

Using mathematical models, the team was able to generate data for lizards with rigid tails, compliant tails, and tailless models to go along with the collected data from the active lizard tail recorded from the high speed camera testing. They then correlated all the data into the graph shown in Figure 3.

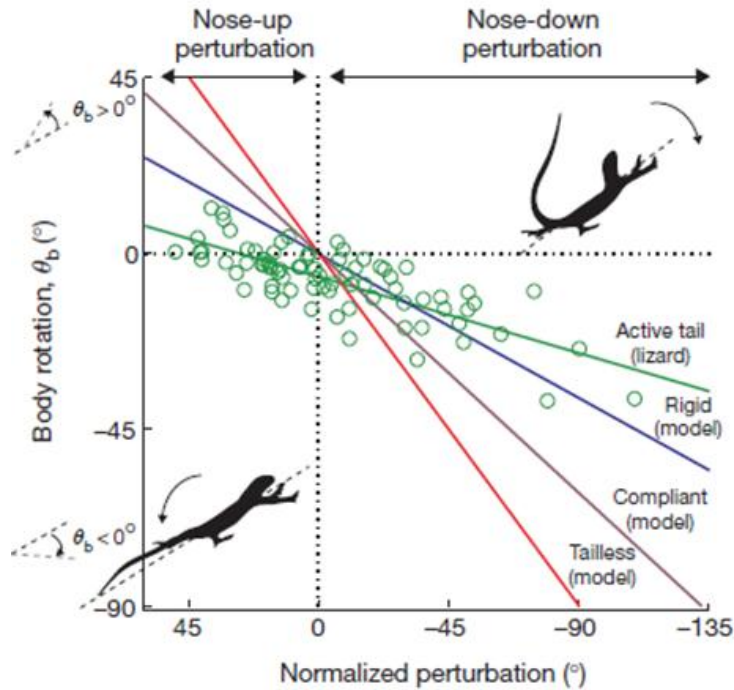


**Figure 3: Sensitivity of Body Rotation to a Perturbation in a Lizard [1]**

In each graph, the slopes of the lines represent sensitivity to perturbations. The greater the slope of the line, the more sensitive the model would be to perturbations. Tail swing is opposite direction than the direction the nose would go. For nose-down perturbation tail would swing upwards. Data shows that the tailless models were the most sensitive to perturbations.

### 3.2 TAILBOT ROBOTIC TAIL

Although inertial stabilization of robots had been studied before, the Tailbot robot was the first to have a specialized tail for continuous inertial stabilization of the body. The team built an agama lizard-sized robot with an aluminum tail appendage. They used proportional-derivative feedback control to stabilize the body angle of the robot. The aluminum rod swung in response to an internal gyroscope which reported the body angle data. Using a ramp representative of a ski-jump, the robot was launched both with proportional derivative control feedback off and then again while on. This test procedure can be seen below in Figure 6a and 6b. The result showed that while the feedback control was on, the swinging of the tail upward incurred 72 percent less rotation than did the robot when no tail control was used. The feedback pictures and graphs are shown in Figure 4.

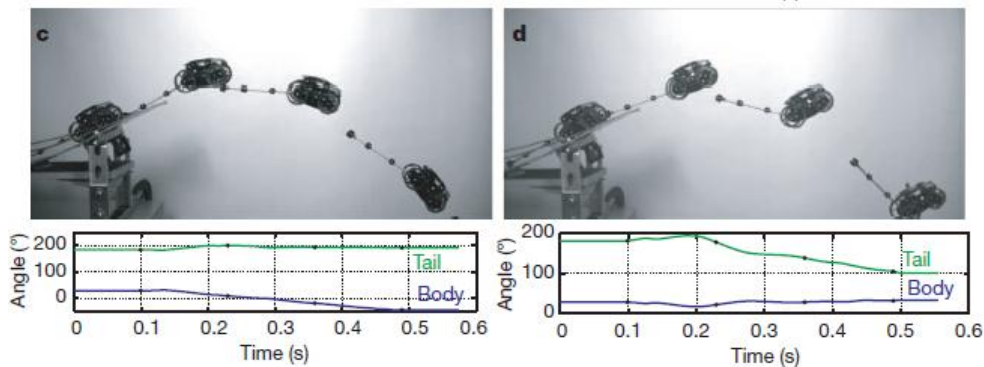


**Figure 4: Robot Tail Effectiveness Testing and Correlation Data [1]**

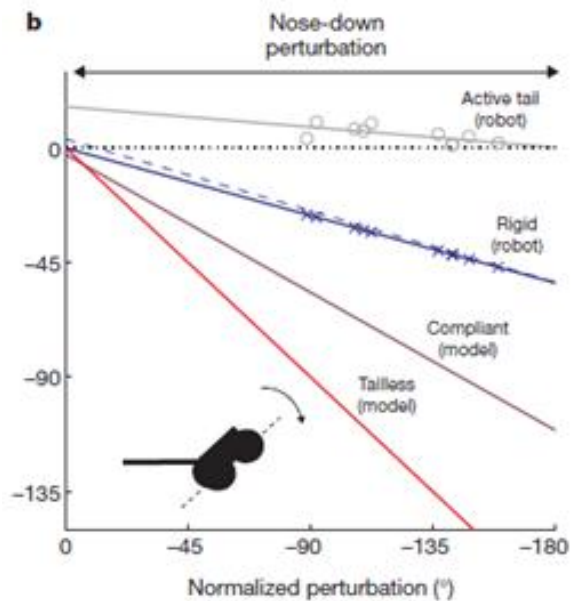


**Figure 5: Tailbot nose-down perturbation based on tail manipulation.**

The data in Figure 4 and Figure 5 show that this tail is effective at overcoming the effects of gravity on the body by moving its tail in opposite direction about 100 degrees over the period of 4 seconds. This is hard to compare to the lizard because its jump combines the added advantage of a front leg jump to overcome the effects of gravity on it. However, in order to compensate for gravity and getting to the top of the platform, the lizard moves its tail angle 1.5 times more than that of the Tailbot in this study; therefore the robotic tail is just as effective in stabilizing unwanted movement as an actual lizard is.

The testing and mathematical models determined that dynamic stabilization could be utilized by a proportional-derivative feedback control device within a robotic body, controlling a

tail-like rod. It was also determined that this robotic tail design was more effective than that of an actual active-tailed lizard; this is shown below in Figure 6. The reason for this is because of added mass to the tip end of the tail attached to the robot. Opposite to that of an actual lizard, the moment control can be greater if the majority of the mass is at a greater length away from the body itself. In a lizard, the majority of the tail mass is at the attachment of the body. This means that greater distance and initial force of tail from the lizard must be used to achieve the relative correction.

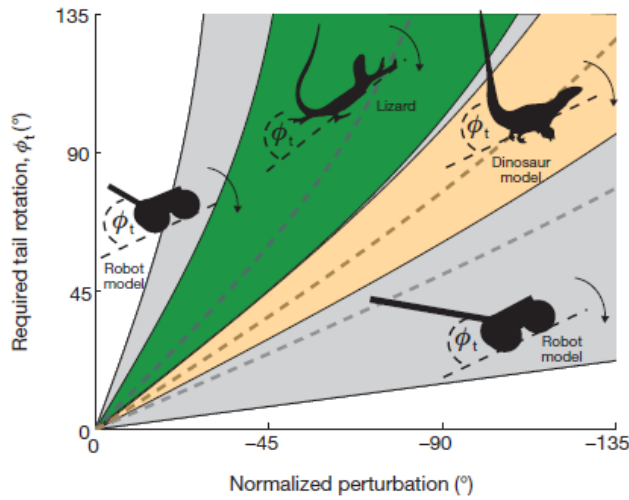


**Figure 6: Tail Effectiveness for Body Perturbations [1]**

Mathematical models of various tail configurations were created and the result concluded that a larger tail would have more effect. The tail effectiveness table is shown above in Figure 6. Upper bound of the grey area is from 5% body mass, 50% body weight where the lower bound is that of 10% body mass, 200% body weight. The actual tested robot data is shown with the dotted black line in the lower bound of the grey area. The ‘Normalized Perturbation’ represents the downward body rotation from the horizontal, where required tail rotation is in the positive angular direction. The tested robot (black dotted line in the lower grey area) counteracted 1.84 degrees of body rotation with each 1 degree of tail rotation. A velociraptor model was also created, and revealed that its tail, if used this way, was more effective than that of their Agama lizard test subjects. They concluded that tails on robotic bodies can have effective control over undesired movement. This research was only conducted in a single plane for nose-up and nose-down perturbations. The equations to their model and other associated information from this study can be found their publication in Jan 2012 edition of Nature Magazine. [1]

### **3.4 ARTICULATED ROBOTIC LIMBS**

As described in their company statement, “Festo is a leading world-wide supplier of automation technology and the performance leader in industrial training and education programs. Our aim: maximized productivity and competitiveness for our customers [2].” They produce many products used in automation, such as for manufacturing. They are a leader in pneumatic, servo-pneumatic, and electric drive technologies, producing systems for product rotation, gripping, holding, and many other processes used automated plants. They advertise over 30,000 catalogue products in automation technologies. They are also a leader in research and development in these automation technologies as well as in other areas; their Bionic Learning Network is one of their research divisions in cooperation with universities and other institutes.

Festo’s Bionic Learning Network “initiative sets out to devise new types of technology platforms and series products through the application of bionics, i.e. the transfer of [animal species] biological principles to engineering. Automated movements can be made more energy-efficient and productive with the help of bionics; this opens up entirely new approaches for industrial practice [2].” The transfer of natural efficiency strategies to automation technology, the testing of the new developed technologies and manufacturing processes, and the development of energy-efficient and bio-mechatronic products are the three objectives set for this initiative.

This bio-mechatronic development in technology by Festo is an evolutionary. Figure 7 below shows three examples from nature that develop into industrial applications.



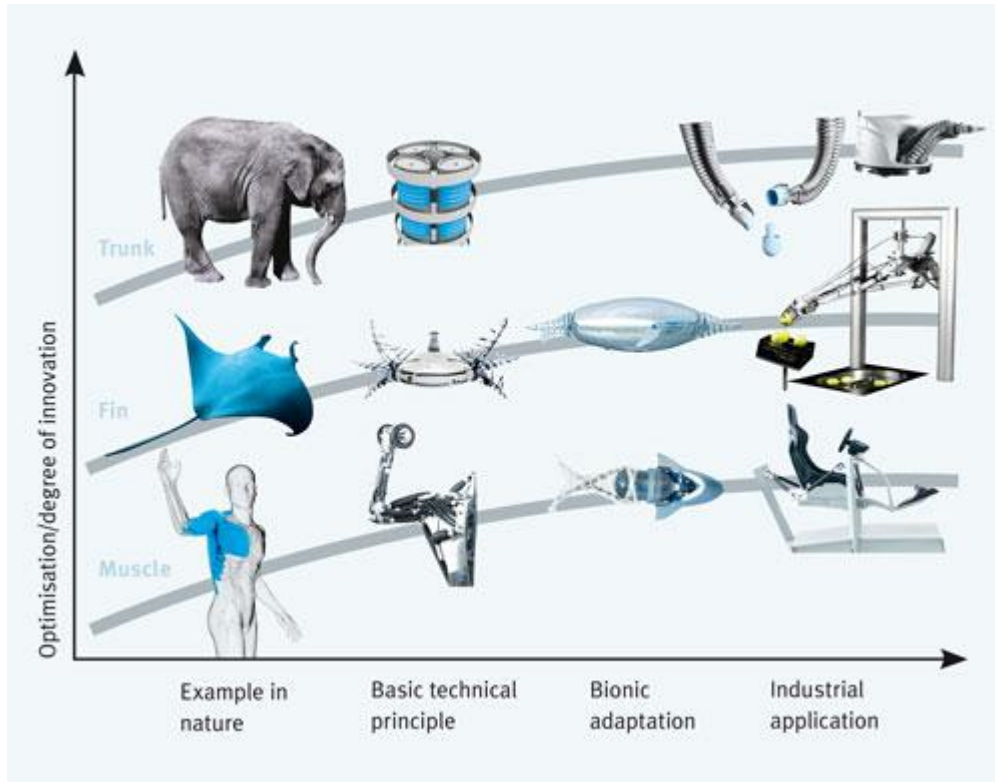


**Figure 7: Bio-mechatronic Robotic Examples of Festo [2]**

Examples such as the shoulder muscle of a human, the fin action of a manta ray, and the functionality of an elephant trunk have all been researched and used in the design of industrial applications for automation technology. A timeline of Festo's biomechatronic developments from its first in 2006 can be seen in the Appendix.

### **3.4.1 Festo Bionic Handling Assistant**

One example of a Festo product is the Bionic Handling Assistant; this can be seen below in Figure 8. Using the biological technology of trunk of an elephant truck, they developed a state of the art robotic handling device. All aspects of the elephant trunk, especially its flexible movement and precise gripping ability, were used in the design and synthesis of the Bionic Handling Assistant.





**Figure 8: Festo's Bionic Handling Assistant [2]**

Just like that of an elephant trunk, the Bionic Handling Assistant is able to extend/contract its length and make precise movements allowing it an unprecedented range of motion. Utilizing air bags throughout the length, and state of the art pneumatic air devices, the handling device extends, contracts, and moves side to side. By varying the air input on one side to another, the arm will curve to its needed location.

The gripper portion of the arm is also derived from biomechatronic technology, but not from that of the elephant. It consists of three fingers which are based on the Fin Ray Effect technology developed by Festo in previous research. It mimics the movement derives from a fish's tail fin. Compared to traditional metal grippers, these grippers conform to the any items surface area, increasing its gripping area. This allows it to grip with less force which enables it to pick up and move even the most delicate items that would normally be crushed with traditional grippers. The gripper can be seen below in Figure 9. [2]

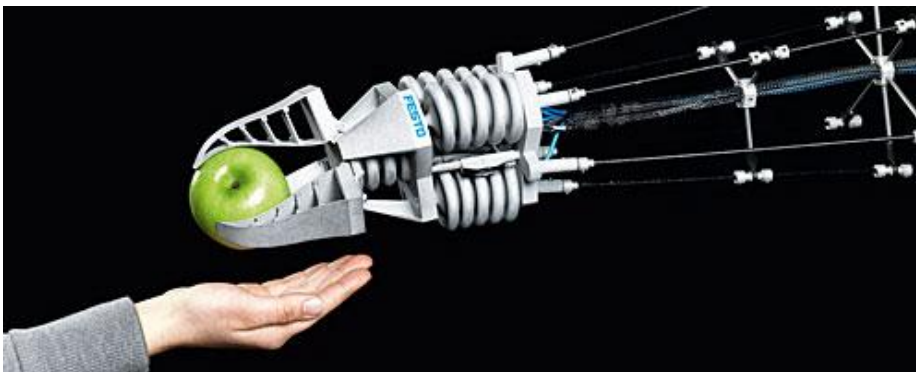


**Figure 9: Bionic Handling Assistant – Gripper [2]**

### **3.6 SUMMARY**

This review of previous literature provides insight and background to many aspects in the tail design process. A review of how lizards move their tails for stabilization was provided. Multiple degree of freedom robotics mimicked after animals are a growing field, especially in the Festo's Bionic Learning Network. From their work in this field we understand some basic control systems that are associated with multiple degree of freedom manipulation as well as synthesis of mathematical modeling techniques.

## **4.0 LIZARD INSPIRED ARTICULATED DESIGN SYNTHESIS**

A simplistic design for a tail needed to be established that mimicked the motion of a lizard on multiple degrees of freedom. To attain this, a design of a spring-mass system with a satisfactory control system to reach the goals was implemented. This section explains the design process and all the concepts that were reviewed and established.

### **4.1 ASSUMPTIONS AND SYSTEM LIMITATIONS**

The first step in the design process was to determine the assumptions and system limitations of the tail design pertaining to this specific project. They are:

- Size of the tail and body should be proportional to that of the agama lizard.
- Size of any prototype tail will not exceed 10 inches
- Control system will utilize electric battery power like that found aboard any RC car.
- All components used/bought/made must be under the allocated budget

Although this list is short, they are necessary to have because time constrains, size limitations, and a budget must be understood when making design decisions.

### **4.2 CONTROL SYSTEM FOR MDOF MANIPULATION**

There are many control systems for multiple degree of freedom robotic manipulation. Each one has its benefits and problems in different situations. Some control systems are designed for accuracy for tasks such as surgical procedures. Other control systems are used for heavy load lifting. There are also different energy sources for these controls such as hydraulic pressure, electric motors, and pneumatic pressure among others. After extensive research, there were two options that were considered based upon the established limitations.

### 4.2.1 Serial Manipulator

A serial manipulator is a robotic system that consists of links connected together through joints that. Figure 10 below shows an example of one

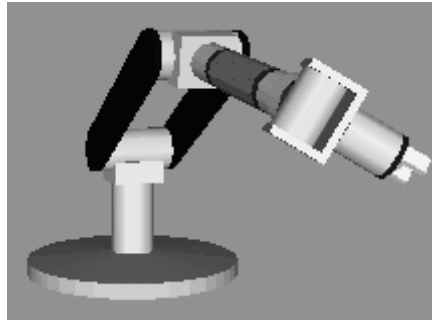


**Figure 10: Serial Manipulator Example**

This type of control system allows for the full range of motion that the tail needs. By controlling each joint by a separate motor, one can manipulate the body to any location. Although this system falls within the limitations, there are many flaws associated with this system specifically pertaining to the desired goals. Having separate control motors at each joint will not be able to provide fast enough manipulation to allow large enough moment changes to the robotic body during uncontrolled motions. Also, because the joints of serial manipulators like this are each in a different plane they only have only two degrees of motion for each. This kind of MDOF motion will not necessarily provide the moment changes we desire.

### 4.2.2 Actuation Control

Actuation control refers to cable driven manipulation system. These are mostly found on gripping robots. Their accuracy can be very well controlled with the combination of cable pulls and base rotation. One example is seen below in Figure 11.

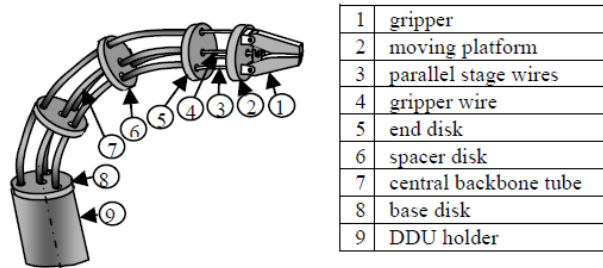


Fig 2. The Distal Dexterity Unit (DDU) composed from a parallel manipulation unit and a snake-like unit.

### Figure 11: Actuation Controlled Robot [3]

For the three dimensional motion required of the lizard inspired tail, there needs to be three separate cables through the system. Cable driven actuation is the most design plausible for our system. Its control is defined by others as snake-like which can be correlated to lizard-like because of its curving motion. Some actuation controlled systems have multiple sections with individual actuators within them. This allows for multiple curves over the entire length of the system. For our tail, however, there will not be multiple motors throughout the tail length; one curving length will be sufficient to attain stabilization control of an unstable body. If there were other actuators within the tail, they could get damaged during regular operation and potentially yield an undesired mass distribution of the tail. Also, high speed actuation, or cable control, is needed to initiate the greatest moment possible from the tail, therefore providing the greatest control to an aggressively moving body. [3] [4]

### 4.2.3 Implemented Design: Modified Actuation Control

After review of the different control systems, a simplified actuation control system was implemented. A three cable pull system was established. No base rotation will be involved, so the degree of total freedom may be hindered by this. Physical prototype testing later on will reveal if this is the case.

### 4.3 MASS DISTRIBUTION

For simplistic design a tail split into four mass segments was implemented. With this distribution, there was enough space and flexibility to mimic the desired movement of the tail as well as keep it within limitations. Figure 12 shown below shows this distribution.

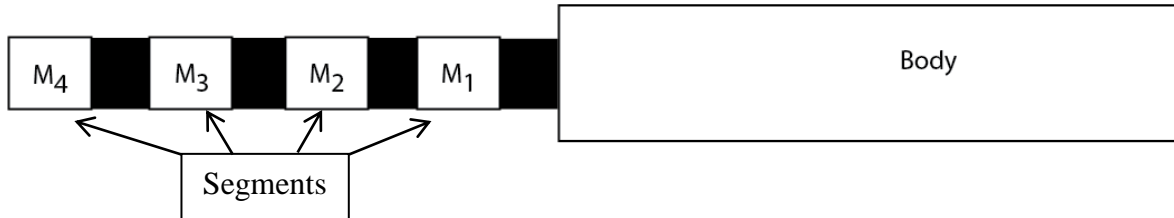


**Figure 12: Mass Distribution of Tail Design**

In lizard physiology the mass distribution consists of  $M_4 < M_3 < M_2 < M_1$ . This is the one aspect of a lizard tail that we will change completely. In order to get the greatest moment change to control an unstable body, the mass moment needs to be as far away from the body as possible, and therefore further in our design we will model for a tail where  $M_4 > M_3 > M_2 > M_1$ . Mathematical modeling will confirm this assumption.

### 4.4 LIGAMENT EQUIVALENT FOR SEGMENT CONNECTIONS

Many concepts for connecting the masses together were reviewed. Properties such as strength, flexibility and ability to rebound (spring-back) were considered. Various types of springs and flexible rods were reviewed.

For springs, both tension and compression springs were reviewed. Simple tests were performed to verify the effectiveness of each type of spring. Small acrylic pieces were laser cut and used to attach to the end of a variety of diameters, k-values, lengths, etc. Below are some of the pictures of this process in Figures 13 through Figure 16.

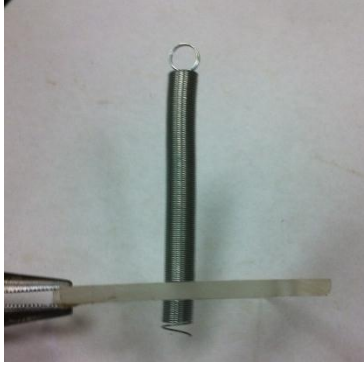


**Figure 13: Tension Spring Attachment Example**

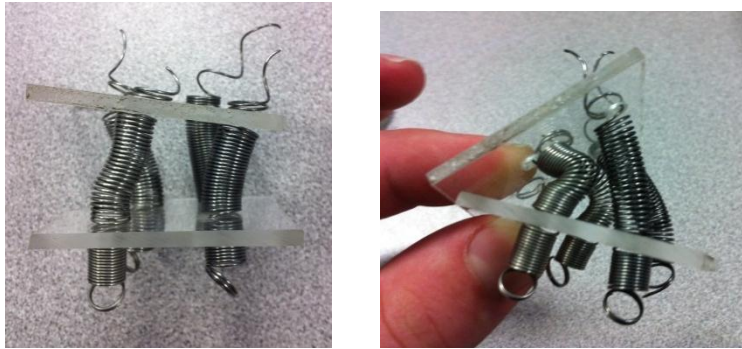


**Figure 14: Quad Tension Spring Example**

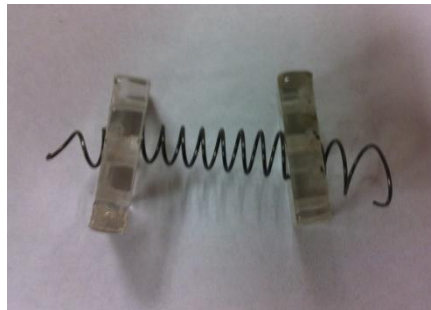


**Figure 15: Compression Spring Example 1**

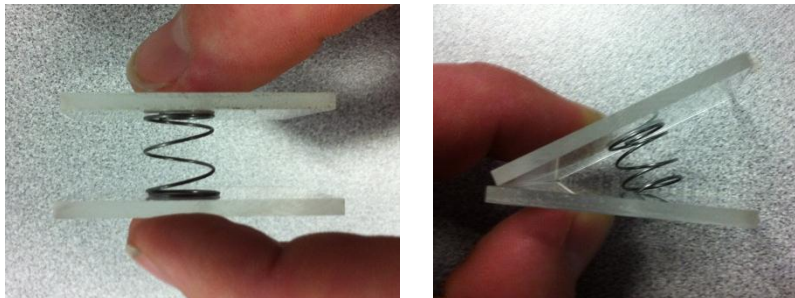


**Figure 16: Compression Spring Example 2**

#### **4.4.1 Tension Springs**

Figures 13 and 14 are examples of tension springs connected with two bodies. Figure 13 shows a possible attachment method of the tension spring to a mass body if designed thin like the plates in an actuated control system as seen in Figure 9 in previous section. Tension springs work well when a lateral force is applied because the spring curves very well when there is one present. However, there was not enough lateral elasticity for the weight of even the small acrylic plate, meaning that while horizontal, it is in constant deflection. Then a four spring system was tried to see if multiple springs together would be able to provide control during manipulation as seen in Figure 14. This was not the case; when multiple tension springs are used, the curvature is not uniform and easy manipulation would not be feasible.

#### **4.4.2 Compression Springs**

Next, compression springs were tested. Figure 15 shows a cone shaped compression spring. There was no apparent difference between the cone shaped spring and a regular cylindrical spring in terms of effectiveness or deflection properties. The compression spring performed well during lateral manipulation. While under lateral manipulation, there was enough elasticity due to the side compression for the plate to spring back to about where it came from. Gravity does create a small amount of permanent deflection. This was a promising discovery as elasticity back to original state was a property desired of a prototype tail. Figure 16 shows a regular cylindrical compression spring which was glued to the surface of the acrylic and then tested. This demonstrated a wider spring with a low k-value and great flexibility; the deflection properties can be seen through the side by side comparison.

#### **4.4.3 Flexible Rods**

The rods that were purchased for design concepts were tested with hand strength. Small plastic and fiberglass rods were purchased for testing. The plastic ones were made of soft plastic, and were hollow and flexible. However, they became indented instead of making a curved shape when a force was applied; therefore it was concluded they were undesirable for this application. The fiberglass rods did not provide enough deflection even at full human strength to mimic the shape that a lizard tail would make during stabilizing. The required forces would have to be too great to get the desired motion if the rod was used as the connection of the masses for the



stabilization tail. Compared to the springs, a rod connection would feed through each mass section whereas a spring system would connect individual springs between the masses.

#### 4.4.4 Implemented Ligament Connection

After review of all materials, the compression springs were selected as the connectors for the tail mass sections. The compression spring has the ability to rebound while still being flexible and strong. The forces required to manipulate the compression springs laterally to maximum deflection are achievable with standard robotic motors. Therefore, compression springs will be used to connect each mass together. Location of the compression springs and how many to use on each has yet to be determined.

#### 4.5 SEGMENT DESIGN

In order to incorporate all of the design concepts implemented so far, the mass section needed to be designed to fit with all the previous concepts. The three cable control system, four part mass distribution, and compression springs needed to be brought together with this piece for a prototype design. The mass section was based upon the plate design like that of the snake-like actuation controlled robot. Also, the section needed to be designed to accommodate two different spring layouts. The first layout was single compression springs straight down the center of the masses while the other was a three spring system where each spring will act as a channel for the cable. The design is shown below in Figure 17

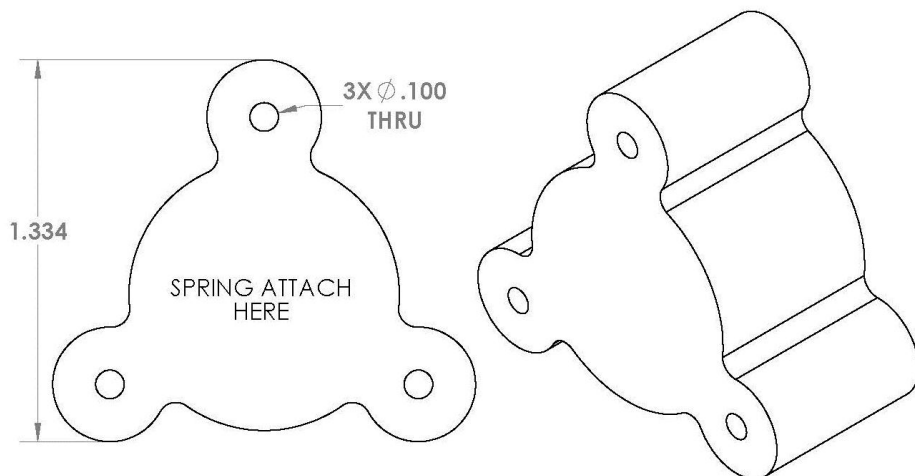


**Figure 17: Mass Section Implemented Design**

The three holes at each corner of the piece are arranged on an equilateral triangle. This allows for even control from all axes. There is sufficient material around the edges of each thru hole in order to attach springs.

#### **4.6 SUMMARY**

For each design component, all possibilities were considered and researched for their potential performance in regards to the goals of this project. Iterations were made when necessary if a poor decision was made. A final selection of all design concepts was decided and then implemented into a physical working prototype. Iterations to some of the previously selected components were made once testing of the working prototype began. This analysis and the changes associated with iterated components are discussed within section 6.0 during prototype fabrication.

## **5.0 MODELING AND SIMULATION**

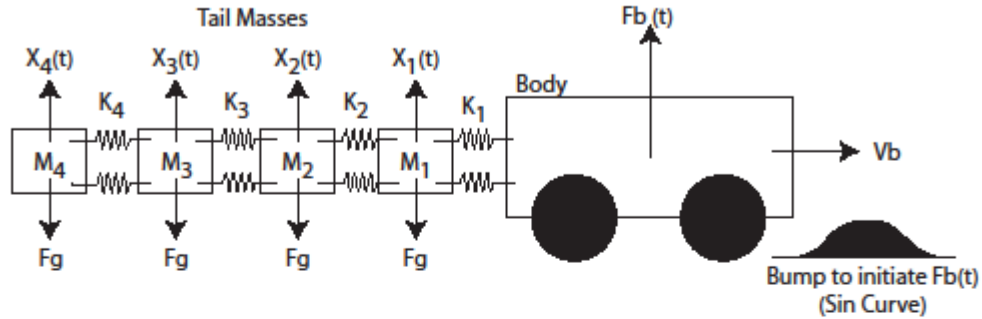
There were many models involved in mathematically determining the feasibility of a lizard inspired tail for purposes of dynamic stabilization of robotic bodies.

### **5.1 VIBRATION ANALYSIS**

After the four segment distribution was decided, the first feasibility study we conducted was to determine if a tail of this design would be able to withstand vigorous motion of a robotic body at a constant velocity over a rough surface; a method for finite element analysis of various tail designs. This was determined by using a modal vibrational analysis for a linear multiple degree of freedom (MDOF) system. The math model was made to input infinite tail designs for the four segment system only. Any variations in mass and spring constants could be used within the final model. Figure 18 shows the free body diagrams associated with the vibrational analysis of tail design. Even though the implemented tail incorporates a one spring system, the dual spring system mimics the tail in tension due to the control strings. The Newton D’Alambert approach was used for this analysis.

### 5.1.1 Free Body Diagrams

Free Body Diagrams and Associated Equations



Equivalent Free Body Diagrams (Newton D'Alembert Approach)

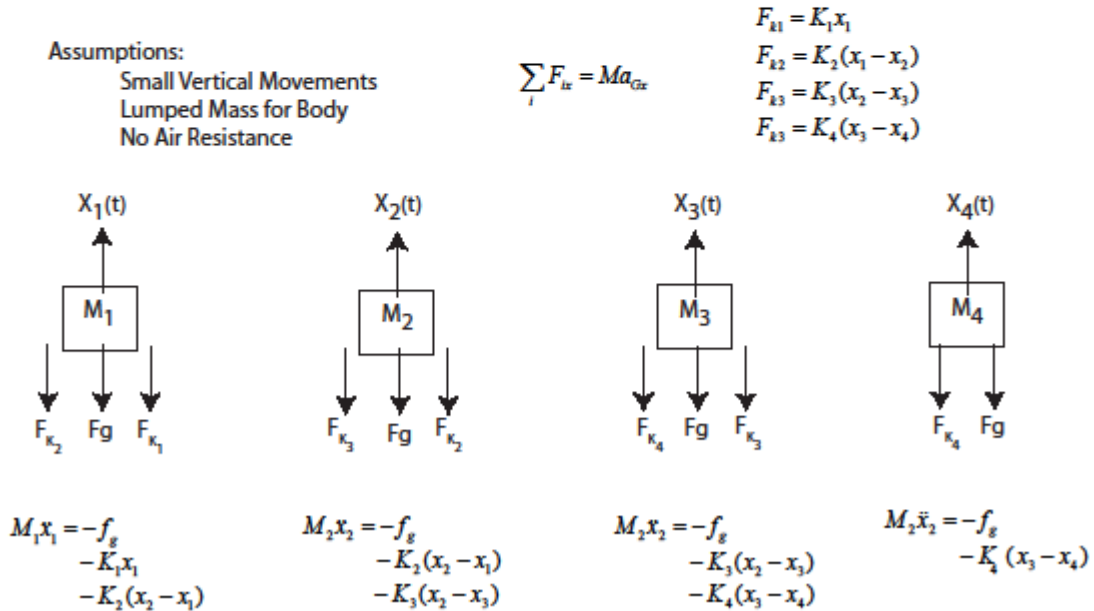


Figure 18: Free Body Diagrams and Equations for Modal Analysis

The free body diagrams in Figure 18 show equivalent force directions for this vibration. Although the springs are connected horizontally, the motion of the body vibration is in the vertical direction. Therefore, the two springs connected on each mass will hinder vertical motion using a proportional combination of tension and compression from each. This is why we assume each double spring is modeled as one vertical spring. This simulates the tail while it is in great tension from the control cable connecting the last mass (M4) to the body; this would be true when the tail is connected to its control system during.

### 5.1.2 Assumptions

There were some assumptions made for the optimization of this Initial Value Problem.

1. While in great overall tension due to the control system, the tail is assumed to be horizontal compared to likely vertical displacement between M1 and M4 due to gravity.
  - a. \*\*the model can accommodate this change with varying initial conditions. Due to simplicity of this initial model, all initials will be set to zero.
2. Instead of rotation about each mass, we are strictly looking at the vertical displacement, therefore assuming that the tension in the system is great enough to hinder rotation of each mass.

For this modal analysis, units are not analyzed because we are assuming normalization. Changing coefficients of force does not change the shape of the output graph. Also, keeping  $K_i/M_i$  (spring constant/mass value) proportional does not affect the shapes of the graphs. Estimation for the k-values and mass values are based upon assuming a k-value of 65 which was decided based upon a maximum displacement desired of about 0.06. If you put units on this normalization, then K-value of 65N/m will yield about 6 cm of maximum deflection in each direction.

### 5.1.3 Initial Value Problem

Formulation of the free body diagrams yielded an Initial Value Problem as follows:

$$M\ddot{x} + Kx = F_b(t)$$

$$M = \begin{bmatrix} M1 & 0 & 0 & 0 \\ 0 & M2 & 0 & 0 \\ 0 & 0 & M3 & 0 \\ 0 & 0 & 0 & M4 \end{bmatrix} \quad K = \begin{bmatrix} K1 + K2 & -K2 & 0 & 0 \\ -K2 & K2 + K3 & -K3 & 0 \\ 0 & -K3 & K3 + K4 & -K4 \\ 0 & 0 & -K4 & K4 \end{bmatrix}$$

$$x(0) = 0 \quad \text{and} \quad \dot{x}(0) = 0$$

$$F_B(t) = \sin(2\pi t) \quad (**\text{simulates 2 bumps of magnitude 1 every second})$$

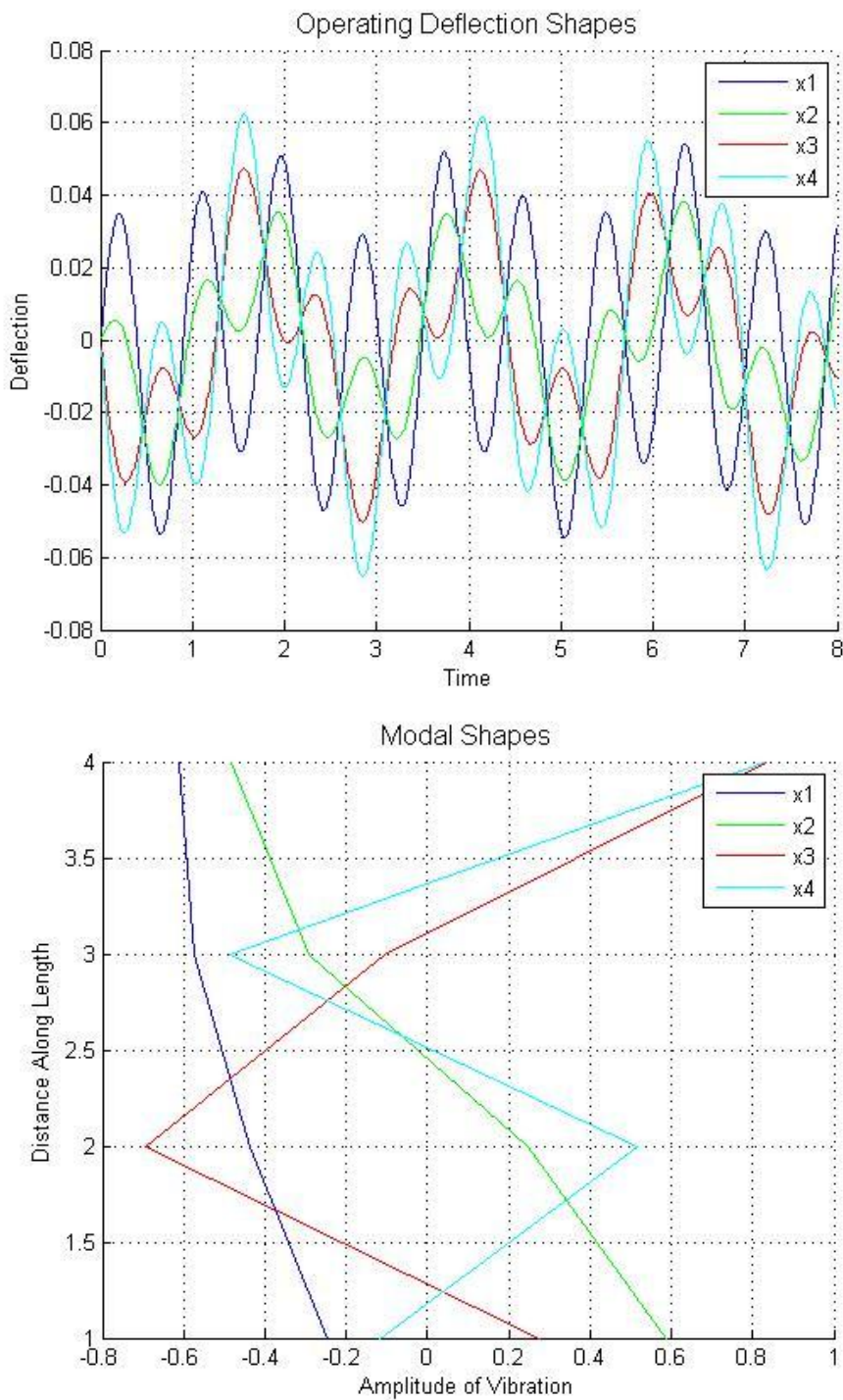
There are many steps to vibrational modal analysis which are explained within Appendix 1.3 via flow chart and step by step mathematical equations. The Matlab code associated with this analysis also in the Appendix.

Three different mass distributions of a tail were assumed for this analysis. One mimics the distribution of an agama lizard, the test subject of UC Berkeley research, and two others mimic possible robotic tail designs; one of them being the direct opposite of the lizard distribution.

#### **5.1.4 Operating Deflection Shapes and Modal Shapes**

Figure 19, 20 and 21 display three different possible tail mass distributions. Figure 19 displays the vibration for actual lizard tail distribution. Figure 20 shows the data for the exact opposite of the lizard tail; shows ‘backwards distribution’ of an actual tail. Figure 21 shows analysis for heavy tail-end mass with equal smaller masses being distributed evenly through the other three. This mimics a design like UC Berkeley’s Tailbot except with the multiple degree of freedom movement capability throughout the entire length of the tail.

$M1 = 2; M2 = 1.5; M3 = 1; M4 =$  
 $M_4$ 
 $M_3$ 
 $M_2$ 
 $M_1$



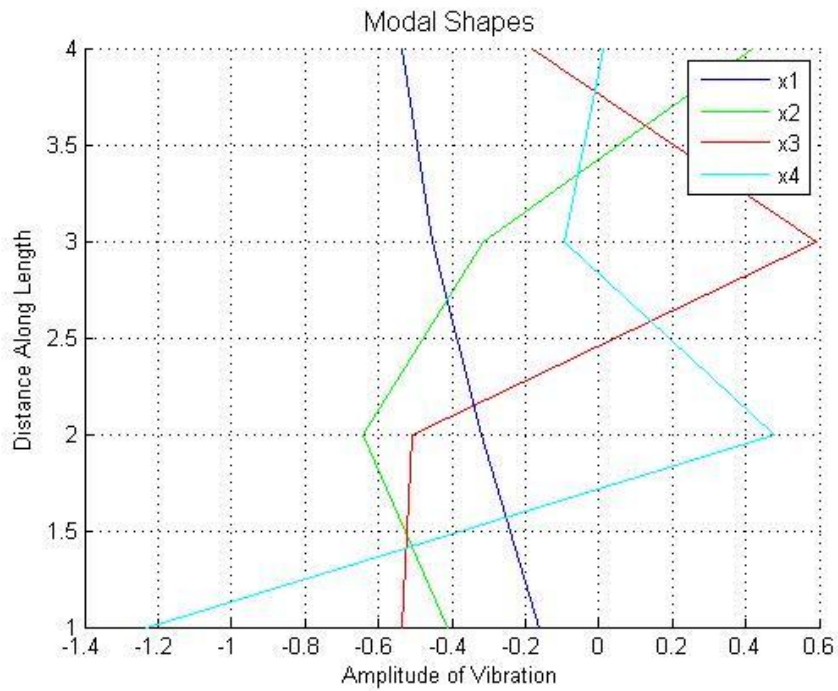
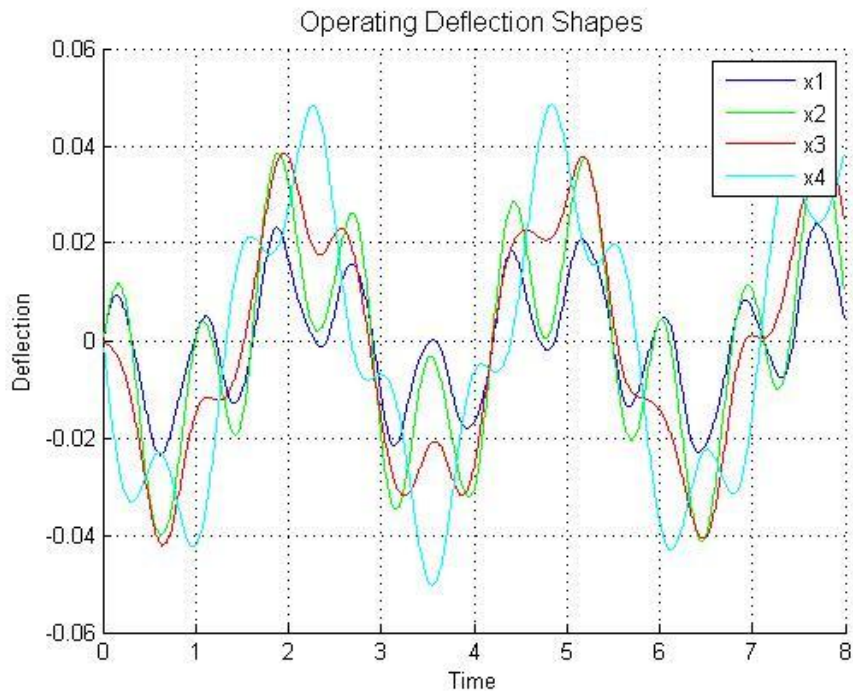
**Figure 19: Lizard Tail Vibration Analysis**

Figure 19 for lizard-mass-distribution shows that there is even distribution of the vibrations caused from the bumps of the moving body. The ODS graph shows that the amplitude of vibration is about the same for all masses throughout the body. This evenly distributed output is attributed to the heavy mass at the front with lower mass at the end.

This is confirmed by the modal shapes graph as well. Amplitude changes in the vibration are low in mode x4, varying from only -0.5 to 0.5 through the center of the length with a higher output at the end of 0.8 which is to be expected to a small whipping of the low mass from the momentum of the traveling vibration. Also, distribution of the various displacements is even throughout the length of the tail as they all have the same frequency of overall vibration.



$M_1 = 0.5; M_2 = 1; M_3 = 1.5; M_4$  M<sub>4</sub> M<sub>3</sub> M<sub>2</sub> M<sub>1</sub>



**Figure 20: Second Vibrational Analysis (Opposite Lizard Tail)**

Figure 20 shows the effects of starting light and ending heavier through comparison with the previous analysis. Through the OPS graph we can see that the masses one, two, and three are moving more closely with each other. This combined movement of the three masses is equally offsetting the deflection of the larger fourth mass.

In addition, this distribution creates a whip motion which can be seen from the modal shapes graph. The movement of  $x_4$  from 1 to 2 shows a larger amplitude switch in same time as compared to that of the lizard distribution. This modal shape shows that the spring system reaches its maximum and controls the section by bringing it back from 0.4 to -0.01 and then it continues back to positive amplitude.

$M1 = 0.5; M2 = 0.5; M3 = 0.5; M4$  
 $M_4$ 
 $M_3$ 
 $M_2$ 
 $M_1$ 
 

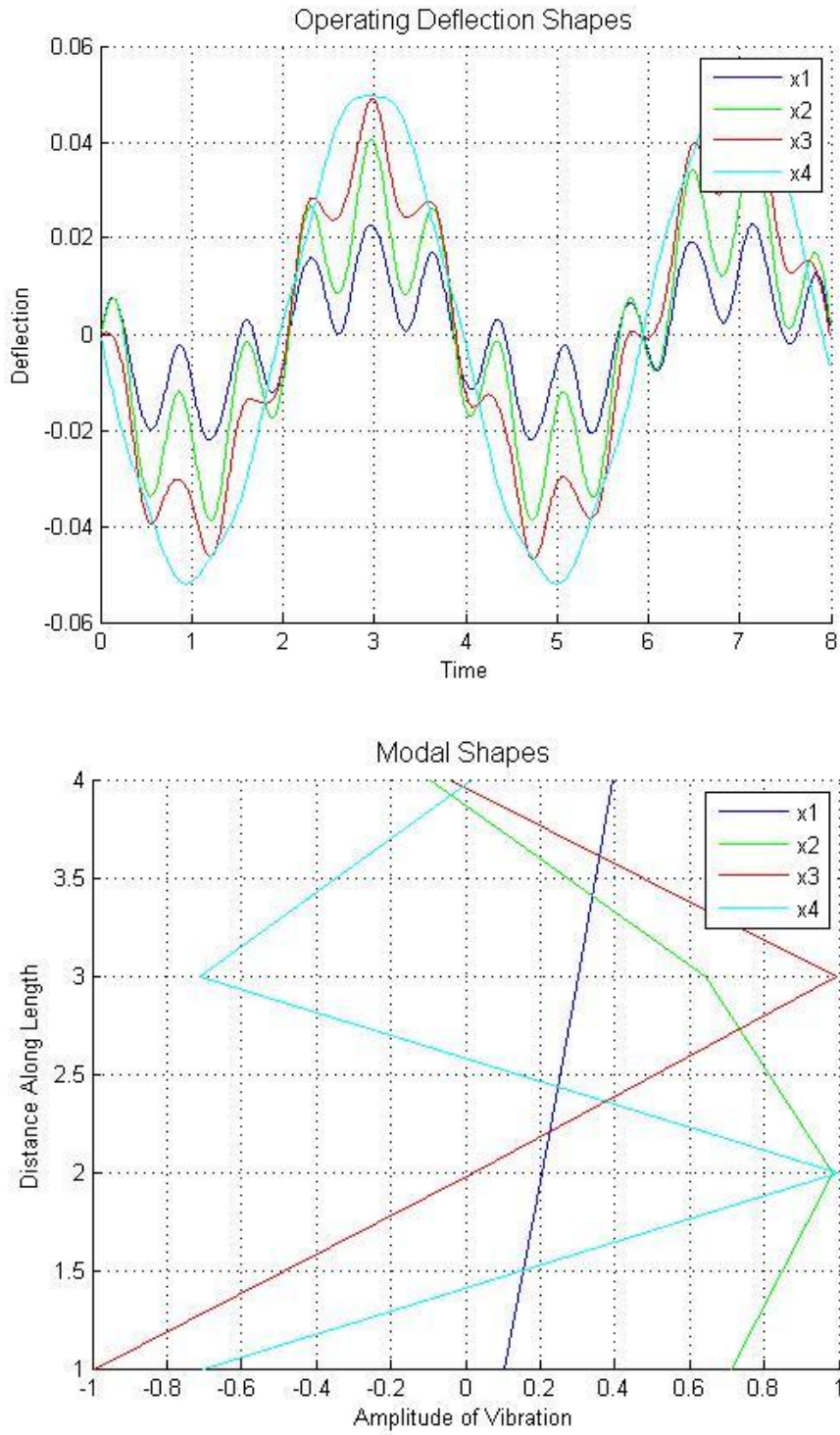


**Figure 21: Third Vibrational Analysis (Heavy M4)**

Figure 21 shows the modal analysis for tail section where M4 is 12 times as great as the mass of the rest of the sections. The Operating Deflection Shapes show resonant behavior, especially for the small masses as they are in high frequency vibration through the whole system while displacing as compared to M4 shape. The Modal Shapes confirm this resonance. X3 and X4 as they are experiencing almost the same amplitude shift from distance 1 to 2, meaning that one is affecting the other creating undesirable amplitude shifts. Also, x4 and x2 are resonating at distance 2 showing that the maximum amplitude of x2 is being influenced by x4 and then finishing at amplitude 0 at length 4.

### **5.1.5 Vibrational Analysis Summary**

The provided tail models are three variations of unique tail designs that can be analyzed by the Matlab model created. Although analysis of each of them is provided, it does not mean that these are optimal or plausible designs for an actual robotic tail though this model. What this vibration system does provide is an insight into the effect of an aggressively moving body has on the tail. This needs to be understood before understanding how a tail can affect a body during maneuvers. The effective vibration of the body on the tail will play a role in a tail's ability to dynamically stabilize the body which it is attached to. If a tail is not stable on its own while attached to a moving body, then it will not be effective for dynamic stabilization or could be damaged due to resonance.

The model was created using Matlab and all of the code is displayed in the Appendix. The code was only designed for a four segment mass system. However, if the original matrices are edited correctly it can be converted to infinite by changing the value of the 'i' in all the IF loops. Also, the initial force curve can be updated; the only problem associated with this is the code for ss\_NHS will have to be changed due to the change in 'Fb(t)' in the Initial Value Problem. Ss\_NHS refers to the homogeneous solution of the Ordinary Differential Equation. Changing this to a different function changes the steady state solution during the modal analysis.

## **5.2 MDOF TAIL MODELING**

A goal of this project was to model a tail on all degrees of freedom and understand how the changes in shape would affect the body it was attached to. There has not been any published works that incorporate manipulation of a segmented body like this on a three dimensional area, so a mathematical analysis had to be created from scratch.

### 5.2.1 Vector Rotation

Vector rotation about an axis was the basis for the first model created to mimic the manipulation of a tail over all degrees of freedom. Using a finite number of vectors in an array to model the length of a tail we could rotate each a small amount to get a desired curve. Figure 22 shows a graphic depicting this process.

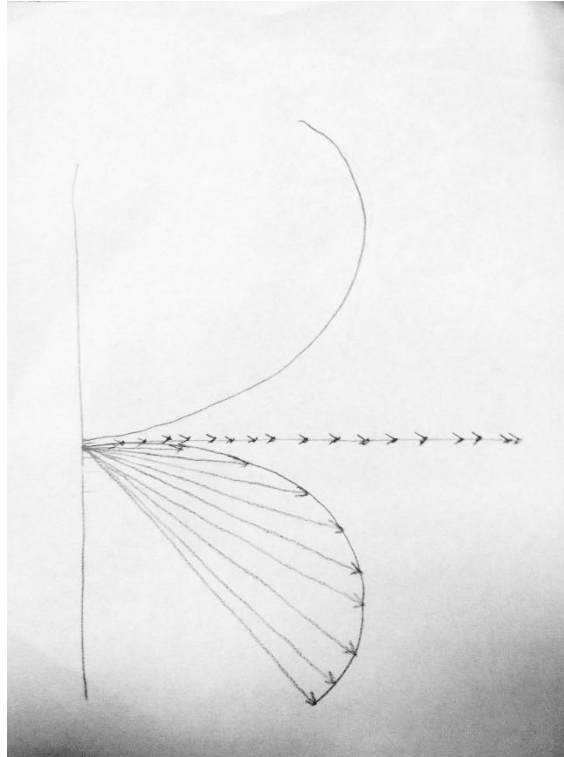


**Figure 22: Visual Example of Vector Rotation**

This figure shows vectors starting on the x-axis, each grounded on the origin. They are then rotated about the z-axis. Determining the angle of the largest vector rotation, we can deduce an equation to mimic a proportional rotation for the rest of the vectors as well. Shown here is just about the z-axis. After this first rotation, we can then manipulate the vectors to rotate about the x-axis and then, in turn, about the y-axis to any desired location. Setting up a function for this process was deduced from Rodrigues's vector rotation formula

$$\mathbf{V}_{rot} = \mathbf{V}\cos\theta + (\mathbf{K} \times \mathbf{V})\sin\theta + \mathbf{K}(\mathbf{K} \cdot \mathbf{V})(1 - \cos\theta)$$

Where  $\mathbf{K}$  is a unit vector describing the axis of desired rotation,  $\theta$  is the desired angle in radians, and  $\mathbf{V}$  is the original Vector. [5]

Matlab code was built for this analysis and graphics were synthesized for design review. The Matlab code can be seen in the Appendix [6]. Figure 23 depicts the line generated by vectors

1 to 5 (stepping every 1), mimicking the motion of the four part tail design. First it is rotated about the Y-axis, then Z-axis, then X-axis all at  $-\pi/3$  radians.

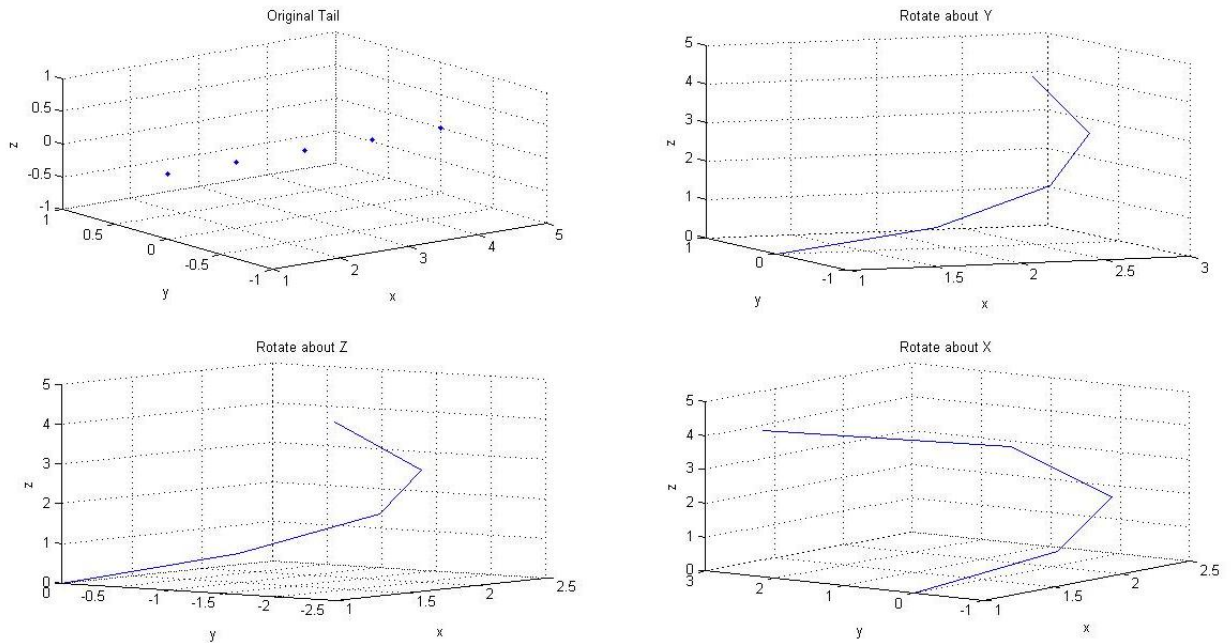


**Figure 23: Vector Rotation of Tail; Matlab Graphs**

All inputs within the code are easily recognizable and labeled according to their purpose. Anyone would be able to use this code to experiment with manipulation properties based upon the Rodrigues Vector Rotation theorem. Also, the code was set up to ensure that the base of the manipulated tail always started from the origin. This would allow for calculations of moments to be about that one point. Effective rotations due to moments of inertia from a specified movement could be explored with a model like this

Design review of this mathematical model revealed some issues with the accuracy. During the rotation of vectors about an axis, the distance between the endpoints changes. This means that a constant tail length is not kept through the rotation processes. This was not taken into account during initial design of the model. Time constraints for this project did not allow for fixing this problem. However, the development of this code achieved a way to model multiple degree of freedom movement.

## 6.0 PROTOTYPE DESIGN

With all of the initial design components decided upon, creation of the physical prototype model for testing was the next step in the design process. The first model was constructed, tested, and then analyzed for its potential effectiveness as a lizard like stabilization tail. Flawed components were reviewed and redesigned; then a second prototype was created, tested and analyzed.

### 6.1 FIRST PROTOTYPE

Figure 24 shows the first prototype model created. Solidworks was used to design the mass sections and then a Rapid Prototype Machine was used to three dimensionally print the model. This method was used for economic considerations because it is cheaper than using metal on CNC machines and other methods of prototyping parts.

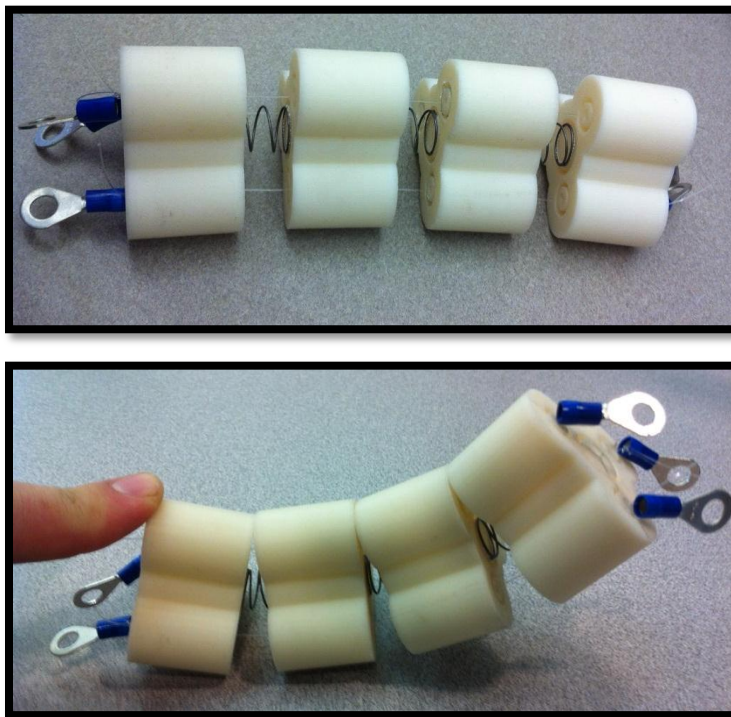


**Figure 24: First Prototype**

For this model, 0.0660” springs were used, with k-value of about 1.5 lbf/in. The diameter of the springs was 0.635” with a wire thickness of 0.025”. The rapid prototype mass sections were 1.5” x 1.5” x 1.5”. They were not weighed as the review of this prototype was for analysis of motion control only. The springs were attached to the mass sections using super glue. High



gage fishing line was used as the cable. Each line was attached to finger pull ends. Manipulation could be controlled by pulling on end of the cables. Gloves and safety goggles were used during the building of this prototype to ensure safety.

### **6.1.1 Design Review**

A design review was conducted on the first physical working prototype. To begin, the control system, designed based upon actuated cable driven robots, was tested. By pulling the various cables, a curved shape was achieved as seen in Figure 24. However, the limitation of the motion was due to the mass sections hitting each other. The curvature achieved during manipulation was in the desired shape; however the maximum displacement was much less than expected. Also, it was determined that the limitations of the degree of curve based upon the shape of the mass section. The maximum deflection was greater while pulling one cable than it was while pulling two at a time.

Positive design characteristics were the centralized spring chain, which allowed for desired MDOF movement, low force requirement during the cable pull, and desired elasticity back to the horizontal position. However, there were flaws with this first prototype too. The mass sections were too thick and the springs were not long enough to get the desire range of motion. Second design will take this into consideration and components will be redesigned to reflect this review.

### **6.1.2 Spring Location Iteration**

After the review of the centralized spring attachment, the model was disassembled to test the effects of the three spring connection system as discussed earlier. It was determined that the distribution of a three point spring system provided the same movement as the centralized single spring. However, the forces required for manipulation during cable pulling became greater. This was because of a combination of compression and tension in the springs during manipulation. While pulling one cable, the spring in line with that cable would compress all the way to its maximum displacement. At the same time, the two springs on the opposite would be undesired tension. Although the tail achieved desired motion, the forces were greater than that of the single centralized mass system. Therefore, the single centralized mass connection system was implemented.



## 6.2 SECOND PROTOTYPE

For this iteration, a new mass section was designed to incorporate only the centralized spring connection system to minimize size. The length of the springs was increased with a new assumed k-value of about 3 lbf/in and the thickness of the section was reduced to 0.700". The same cable system used in prototype one was used again.

### 6.2.1 Design Review

By implementing the changes from the review of the first prototype, drastic differences are seen in the control aspect of this second design. The curving motion was in the desired shape when pulling on the cable, but with greater displacement. Also, MDOF movement was possible through the various pulling of different cables. The Figure 25 and 26 shows photos of the second prototype during MDOF manipulations.



**Figure 25: Prototype Two Manipulation Examples**

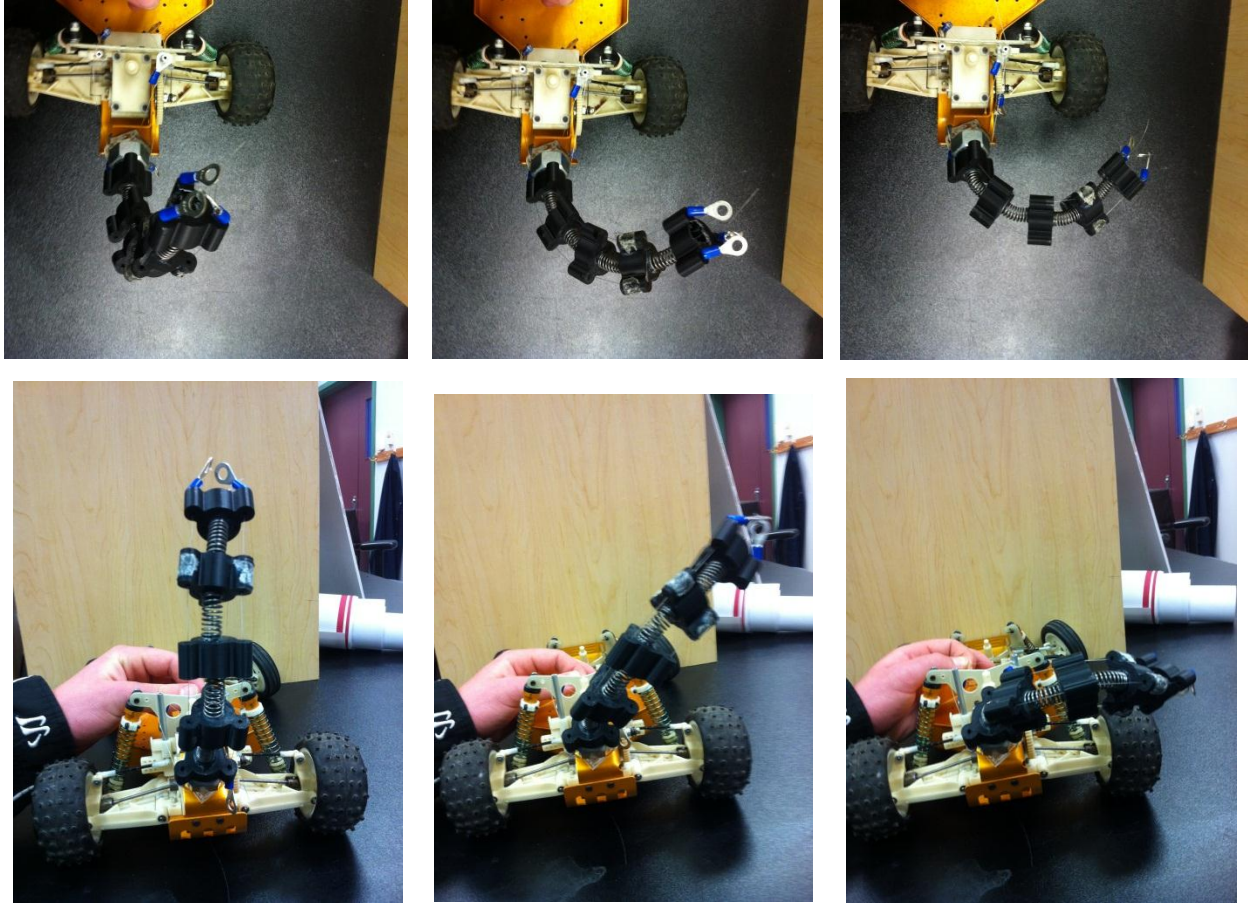


**Figure 26: Top and Back View of MDOF Movement**

Figure 26 shows a potential rotational control mechanism for axial rotation about the center of the robot during an undesired roll. There are infinite possibilities of control with this system.

As compared to the first prototype, this iteration had the same curving shape but on a greater displacement. The mass sections were not this limiting factor for this prototype, but instead the springs and the cable tensions were the limiting factor of motion.

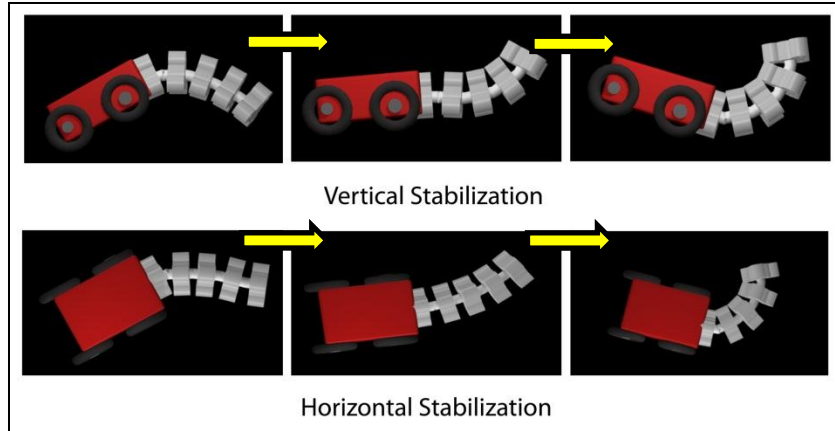


**Figure 27: Modeling of Tail Stabilization Technique**

Figure 27 above show the process for which this type of tail would stabilize a robotic. The movements of the tail could control the rotation of the body in all directions. Here, vertical and horizontal stabilization is reviewed, but this tail design would be able to control these simultaneously with its articulated design. This prototype and hand pulling of the cables were all the time constraints allowed for. Attachment of the cables to servos is an ongoing process and once done, the body can be sent of a ramp to see the tails effectiveness at stabilizing the body it is attached to.

## 7.0 PROJECT ACCOMPLISHMENTS AND DISCUSSIONS

The stated goal of this project was to design and model a lizard-inspired tail for the use of dynamic stabilization for aggressive moving robots. This was a very ambitious goal for the timeline for completion of this project. However, great steps toward the realization of the goal were achieved.

A lizard inspired tail design was produced through specific design methods and then fabricated. Also, a working model of the designed tail was created. Manipulation on all degrees of freedom of a lizard inspired tail through a cable pull system was achieved. This validates the feasibility that a tail of this design can be used for its desired purpose. More research and mathematical validation will be needed to validate its actual ability stabilize a body, but for now the motion achieved with this tail design has the potential to do this through multiple degrees of freedom control.

The mathematical model which tests vibration of the tail from normal body stresses was designed. This provides insight into feasibility options of various tail designs. With infinite spring-mass combinations, this model is able to determine the vibrations of certain mass distribution under certain tension from the control system. If the modal shapes do not show any resonance and the operating deflection shapes have desired deflections, a tail of that distribution could be implemented and further tested due to the mathematical validation.

The beginning to multiple degree of freedom motion of a defined tail through vector rotation was accomplished in a Matlab model. When combined with other tail aspects such as mass distribution modeling, centroid motions, and other properties associated with stabilization properties, there is great potential toward the ultimate goal of modeling the entire system.

## **8.0 FUTURE WORK**

There are many future works present with the prototype and mathematical models which can continue from the work already completed. These include both physical modeling, like the completion of the vector rotation code, as well as mathematical models in controls for controlling the manipulation of this tail stabilization device.

### **8.1 PHYSICAL DYNAMICS MODEL: MATHEMATICAL**

In future works, the first step to the continuation of this project would be to optimize the vector rotation code to ensure full tail length and section length to remain constant throughout the various rotations. Once this is complete, mass distribution equations through such methods as elliptical integrals can be done through each vector. Then, properties such as mass moment of inertia and mass centroids can be calculated for all degrees of freedom. These are the important characteristic models to attain because once achieved; the moment swings of the tail over a time interval can be calculated and will provide mathematical insight into the effectiveness of stabilization that a lizard inspired tail like the one designed in this project could induce on a robotic body. The synthesis of a model like this and the modal vibrational analysis would provide enough physical insight into the feasibility of certain mass distributions in tails and their effectiveness for stabilization of an aggressively moving body.

There are also limits that were not considered during the vibrational analysis code creation that could be part of future works. The system is only set up for a four segment system which we just decided upon as being the basis for our feasibility project. By no means have we proven that a four segment distribution is the best. Optimizing the code for any number of segments would provide a greater outlook on optimal design for a tail stabilization structure. Also, the deflection of gravity was not considered and should be added as well

### **8.2 PROTOTYPE MODEL**

The model created during this project was a very simplified model using cheap, economic, and lightweight parts. For future works, different materials and combination methods should be reviewed. Connection of the springs to the masses should be reviewed and improved. The cable system should be reviewed for material selection as well. The ultimate goal is to be able to control the cables with servos and manipulate the tail through data from an onboard

accelerometer. Future works should include the streamlined control of this specific cable system and understand the movements that it makes through the pulls. Connecting this physical information would enable an automated control system for the dynamic stabilization of a robotic. These goals are very ambitious, but every small step toward the ultimate goal will provide further insight into this kind of system.

## 9.0 CONCLUSIONS

The purpose of this project was to determine the feasibility of a lizard inspired tail for the dynamic stabilization of robotic bodies during aerial or aggressive maneuvers. A mathematical model was created to determine the effects of various tail designs. A physical model of the tail design was fabricated and used to determine feasibility of the design and evaluate the mathematical model. Through modeling and prototype development, it was proven that a lizard inspired tail design is feasible for dynamically stabilizing robotic bodies during aggressive maneuvers. Although not proven physically, a tail of this segmented design can be a part of a fast moving robot. The tail design allows it to move on all degrees of freedom. This will allow any undesired motion from a body to be corrected. Unlike Tailbot's straight shaft tail, the articulated design developed during this project has the ability to be controlled dynamically and continuously, and provide orientation correction in pitch, roll and yaw.

## BIBLIOGRAPHY

- [1] T. Libby, T. Moore, E. Chang-Siu, D. Li, D. Cohen, A. Jusufi and R. Full, "Tail-assisted pitch control in lizards, robots, and dinosaurs," *Nature*, vol. 481, pp. 181-184, 4 January 2012.
- [2] Festo, "Bionic Learning Network," Festo, 2012. [Online]. Available: [http://www.festo.com/cms/en-us\\_us/4981.htm](http://www.festo.com/cms/en-us_us/4981.htm).
- [3] K. Xu and N. Simaan, "Actuation Compensation for Flexible Surgical Snake-Like Robots with Redundant Remote Actuation," Columbia University Mechanical Engineering, New York, NY, 2006.
- [4] K. Xu and N. Simaan, "Analytic Formulation for Kinematics, Statics, and Shape Restoration of Multibackbone Continuum Robots Via Elliptic Integrals," *Journal of Mechanisms and Robotics*, vol. 2, February 2010.
- [5] D. Koks, *Explorations in Mathematical Physics*, Springer Science and Business Media, LLC, 2006.
- [6] "Rotate Vector(s) About and Axis," Ismail Hameduddin, 2012.
- [7] Encyclopedia Britannica, "Lizard (Reptile)," Encyclopedia Britannica Inc, 2012. [Online]. Available: <http://www.britannica.com/EBchecked/topic/345004/lizard>. [Accessed 2012].
- [8] L.-W. Tsai, *Robot Analysis*, New York, NY: John Wiley & Sons, Inc, 1999.



# APPENDIX 1: MDOF MATHEMATICAL MODELING

## APPENDIX 1.1: MODAL ANALYSIS MATLAB CODE

Appendix 1.1 Modal Analysis Matlab Code

4/27/12 12:55 PM R:\MQP\Matlab\Modlar Solution Approach.m 1 of 3

```
%% Modal Analysis of Lizard Tail
% Basic analysis on equivalent cart system
% Adapted from Modal Analysis Flow Chart
clear all; clc; close all
%% Set IVP Matricies

m1=.5; m2=.5; m3=.5; m4=3; %kg
c1=0; c2=0; c3=0; c4=0;
k=1; %N/m
k1=k; k2=k; k3=k; k4=k;

M= [m1,0,0,0; 0,m2,0,0; 0,0,m3,0; 0,0,0,m4];
C= [(c1+c2),-c2,0,0; -c2,(c2+c3),-c3,0; 0,-c3,(c3+c4),-c4; 0,0,-c4,c4];
K= [(k1+k2),-k2,0,0; -k2,(k2+k3),-k3,0; 0,-k3,(k3+k4),-k4; 0,0,-k4,k4];
zeta=0; %modal damping ration for all modes (--> C is constnt and zero)

%% Initial Conditions
x1=0; x2=0; x3=0; x4=0;
v1=0; v2=0; v3=0; v4=0;

X0=[x1;x2;x3;x4]; %Initial Displacement Matrix (x0)
V0=[v1;v2;v3;v4]; %Initial Velocity Matrix (xdot0)

% Harmonic Loading Parameter
% Mimics constant velocity
% For given F(t) --> F0*sin(omegaf*t) [Rvector]
f1=1; f2=1; f3=1; f4=1; %#Induces the harmonic load

omegaf=pi;
R=[f1;f2;f3;f4]; %vector for F(t)=F0*sin(omegaf*t)
F0=R

%% Eigen solution
[PHI,LAMDA]=eig(K,M); %PHI--> Modal Matrix; LAMDA-->eigenvalues
PHI_inverse=inv(PHI); %Inverse Modal Matrix

% Modal Parameters
MMM=PHI'*M*PHI;
KKK=PHI'*K*PHI;
CCC=PHI'*C*PHI;
P=PHI'*F0;
% Modal Initial Conditions
etax0=PHI_inverse*X0;
etav0=PHI_inverse*V0;

% Time Integration Parameters
T0=0; TH=0.01; NT=800; duration=T0+(NT-1)*TH;
time=T0:TH:duration;

%% For Loop: i-th Modal Response
for i=1:4
    % Modal Parameters for ith mode
```

```

mi=MMM(i,i);
ci=CCC(i,i);
ki=KKK(i,i);
omegai=sqrt(ki/mi);
pi=P(i);
zetai=zeta;
omegadi=omegai*sqrt(1-zeta*zetai);

% Modal initial conditions in ith mode
etaxi0=etax0(i);
etavi0=etav0(i);
ri=omegai/omegaf;
temp1=1-ri*ri;
temp2=2*zeta*ri;
Ai=F0(i)*pi/ki/sqrt(temp1*temp1+temp2*temp2);
thetai=atan2(temp2,temp1); %amplitude and phase shift
                             %of steady-state response
c1=etaxi0+Ai*sin(thetai);
c2=(etavi0+zetai*omegai*c1-omegaf*Ai*cos(thetai))/omegadi;

ee=exp(-zetai*omegai*time);
ss=sin(omegadi*time);
cc=cos(omegadi*time);
ss_NHS=Ai*sin(omegadi*time);
eta(i,:)=ee.*(c1*cc+c2*ss)+ss_NHS;
end

%% Physical Response
x=PHI*eta;
x1=x(1,:); x2=x(2,:); x3=x(3,:); x4=x(4,:);

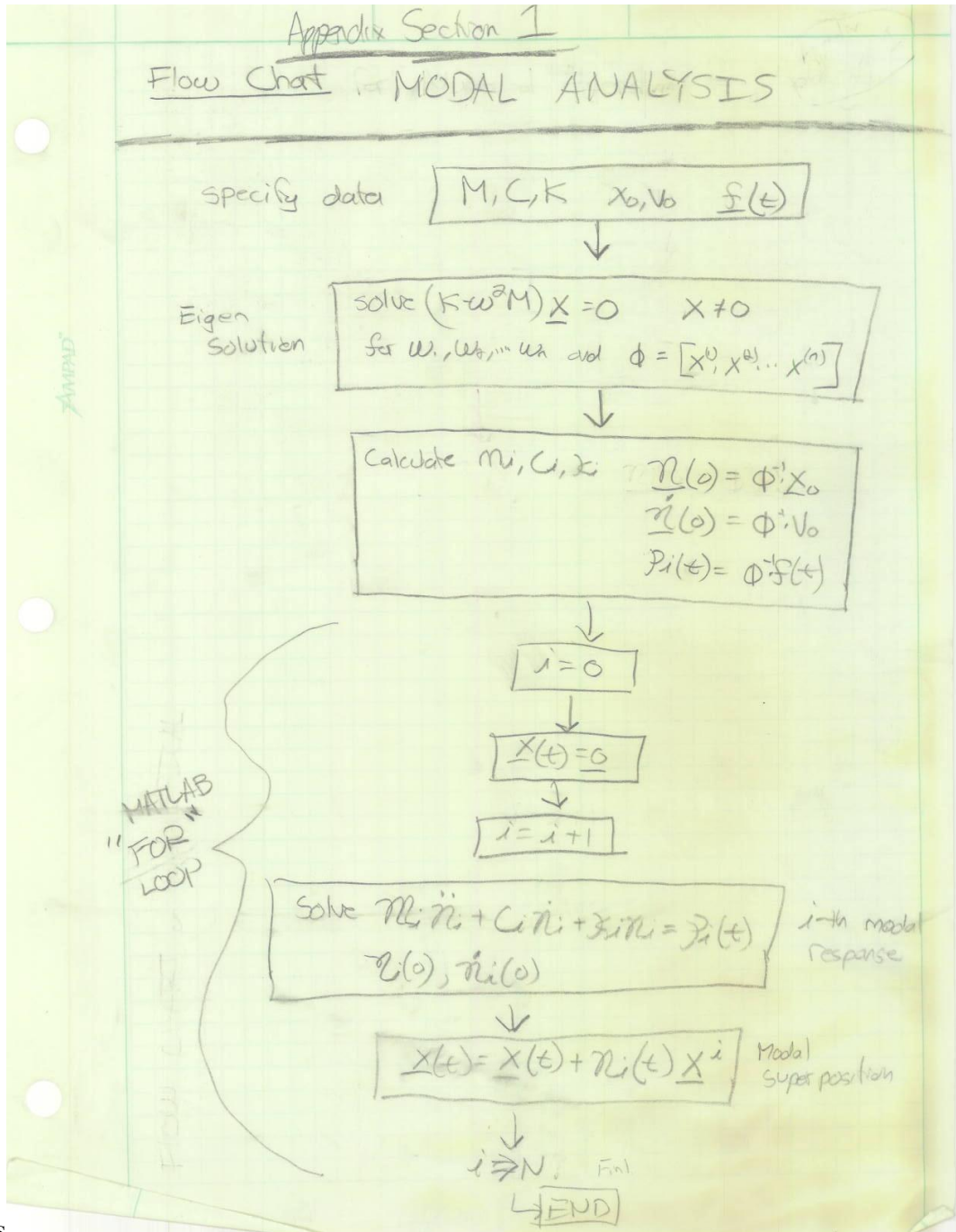
%% Graphical Respresentaion
figure(1) %Individual Shapes
subplot(4,1,1); plot(time,x1),grid on, xlabel('time'), ylabel('x1(t)');
subplot(4,1,2); plot(time,x2),grid on, xlabel('time'), ylabel('x2(t)');
subplot(4,1,3); plot(time,x3),grid on, xlabel('time'), ylabel('x3(t)');
subplot(4,1,4); plot(time,x4),grid on, xlabel('time'), ylabel('x4(t)');

%sinplot=F0*sin(omegaf*time);
figure(2)
grid on; title('Operating Deflection Shapes','fontsize',12)
xlabel('Time'), ylabel('Deflection')
hold on
plot(time,x1,'b'); plot(time,x2,'g');
plot(time,x3,'r'); plot(time,x4,'c');
hold off
legend('x1','x2','x3','x4')
PHI

%% Modal Shapes
PHIt=PHI'
```

```
modal1=PHIt(1,:); modal2=PHIt(2,:); modal3=PHIt(3,:); modal4=PHIt(4,:);
z=1:4
figure(3)
grid on; title('Modal Shapes','fontsize',12);
xlabel('Amplitude of Vibration'),
ylabel('Distance Along Length')
hold on
plot(modal1,z,'b'),plot(modal2,z,'g')
plot(modal3,z,'r'),plot(modal4,z,'c')
hold off
legend('x1','x2','x3','x4')
```

# APPENDIX 1.2: MODAL FLOW CHART AND EQUATION



S

## MODAL ANALYSIS (step 1)

STANDARD GOVERNING EQUATION for MDOF system:

IVP]  $M \ddot{x} + C \dot{x} + Kx = f(t)$       For initial  $x(0) = 0$        $\dot{x}(0) = 0$

Modal Analysis

$x(t) = \sum_{i=1}^n u_i(t) X_i$   
 ↳ physical response

$$M = \begin{bmatrix} m_1 & 0 & 0 & 0 \\ 0 & m_2 & 0 & 0 \\ 0 & 0 & m_3 & 0 \\ 0 & 0 & 0 & m_4 \end{bmatrix}$$

$$C = \begin{bmatrix} (c_1+c_2) & -c_2 & 0 & 0 \\ -c_2 & c_2+c_3 & -c_3 & 0 \\ 0 & -c_3 & c_3+c_4 & -c_4 \\ 0 & 0 & -c_4 & c_4 \end{bmatrix}$$

$$K = \begin{bmatrix} (k_1+k_2) & -k_2 & 0 & 0 \\ -k_2 & k_2+k_3 & -k_3 & 0 \\ 0 & -k_3 & k_3+k_4 & -k_4 \\ 0 & 0 & -k_4 & k_4 \end{bmatrix}$$

$$f(t) = \begin{bmatrix} f_1(t) \\ f_2(t) \\ f_3(t) \\ f_4(t) \end{bmatrix}$$

$f_4(t) = F_0 \sin(\omega_s t)$        $\begin{bmatrix} f_1(t) \\ f_2(t) \\ f_3(t) \\ f_4(t) \end{bmatrix}$

I V P



Basic Principles of Modal Analysis

IVP:  $M\ddot{x} + C\dot{x} + Kx = F \quad x(0) = x_0 \quad \dot{x}(0) = v_0$

↳ Eigenvalue

$\omega_1, \omega_2, \dots, \omega_n$

$\Phi = [x^{(1)}, x^{(2)}, \dots, x^{(n)}]$

$* \underline{x} = \sum_{i=1}^n \eta_i(t) \underline{x}^{(i)} = \Phi \underline{\eta}(t)$

STEP 2

$\Phi^T M \Phi \ddot{\underline{x}} + \Phi^T C \Phi \dot{\underline{x}} + \Phi^T K \Phi \underline{x} = \Phi^T F$

↳ where  $\Phi^T M \Phi = \begin{bmatrix} m_1 & & 0 \\ & \ddots & \\ 0 & & m_n \end{bmatrix}$

↳  $P = \Phi^T F$

$\Phi^T K \Phi = \begin{bmatrix} k_1 & & 0 \\ & \ddots & \\ 0 & & k_n \end{bmatrix}$

$\Rightarrow \eta_i \ddot{\eta}_i + c_i \dot{\eta}_i + k_i \eta_i = p_i(t)$   
 $i = (1, 2, \dots, N)$

← IVP FOR MODAL

Eigen Vectors

$\underline{x}(t) = \Phi \underline{\eta}(t)$

↳  $\underline{x}(0) = \Phi \underline{\eta}(0)$

$\dot{\underline{x}}(0) = \Phi \dot{\underline{\eta}}(0)$

$\Rightarrow \underline{\eta}(0) = \Phi^{-1} \underline{x}(0) = \underline{\eta}_0$

$\Rightarrow \dot{\underline{\eta}}(0) = \Phi^{-1} \dot{\underline{x}}(0) = \dot{\underline{\eta}}_0$

$\eta_i(0) = \eta_{i0}$   
 $\dot{\eta}_i(0) = \dot{\eta}_{i0}$   
 $i = (1, 2, \dots, N)$

## APPENDIX 1.3: VECTOR ROTATION MATLAB CODE

Appendix 1.3: Vector Rotation Matlab Code

4/27/12 12:56 PM R:\MQP\Matlab\vector\_rot.m

1 of 1

```
% Rotates array of 3D vectors by an angle theta about vector k.
% Direction is determined by the right-hand (screw) rule.
% Sourced from Matworks Online Community Database
% Syntax: v_rot = rodrigues(v,k,theta)
% Author: Ismail Hameduddin
% Mechanical Engineering, Purdue University
% email: ihameduddin@gmail.com
% Website: http://www.ismailh.com
% January 2011; Last revision: 2-January-2012

%----- BEGIN CODE -----

function v_rot = vector_rot(v,k,theta)
    [m,n] = size(v);
    if (m ~= 3 && n ~= 3)
        error('input vector is/are not three dimensional'), end
    if (size(v) ~= size(k))
        error('rotation vector v and axis k have different dimensions'),end

    k = k/sqrt(k(1)^2 + k(2)^2 + k(3)^2); % normalize rotation axis
    No = numel(v)/3; % number of vectors in array
    v_rot = v; % initialize rotated vector array
    if ( n == 3 )
        crosskv = v(1,:); % initialize cross product k and v with right dim.
        for i = 1:No
            crosskv(1) = k(2)*v(i,3) - k(3)*v(i,2);
            crosskv(2) = k(3)*v(i,1) - k(1)*v(i,3);
            crosskv(3) = k(1)*v(i,2) - k(2)*v(i,1);
            v_rot(i,:) = cos(theta)*v(i,:) + (crosskv)*sin(theta) + k*(dot(k,v(i,:)))*(1 -
- cos(theta));
        end
    else % if m == 3 && n ~= 3
        crosskv = v(:,1); % initialize cross product k and v with right dim.
        for i = 1:No
            crosskv(1) = k(2)*v(3,i) - k(3)*v(2,i);
            crosskv(2) = k(3)*v(1,i) - k(1)*v(3,i);
            crosskv(3) = k(1)*v(2,i) - k(2)*v(1,i);
            v_rot(:,i) = cos(theta)*v(:,i) + (crosskv)*sin(theta)...
                + k*(dot(k,v(:,i)))*(1 - cos(theta));
        end
    end
end

%----- END OF CODE -----
```

```

%% Vector Rotation about an Axis
% Micahel Berlied
clear all; clc;
global v k theta
L=5; %tail length
dV=1;
y1=dV:dV:L;
nv=length(y1);
%% Setup Proper Matrices
vmatrix=zeros(length(y1),3);
%setup vectors in matrix form
for n=1:nv
    vmatrix(n,1)=y1(n);
end
% setup rotation axis matrices
kmatrixX=zeros(nv,3);
kmatrixY=zeros(nv,3);
kmatrixZ=zeros(nv,3);
for n=1:nv
    kmatrixX(n,1)=1;
    kmatrixY(n,2)=1;
    kmatrixZ(n,3)=1;
end
%setup rotation angles
thetamaxX=-pi/3 %radians
thetamaxY=-pi/3 %radians
thetamaxZ=-pi/3 %radians
tmatrixX(1)=0; tstepX=thetamaxX/(nv-1)
tmatrixY(1)=0; tstepY=thetamaxY/(nv-1)
tmatrixZ(1)=0; tstepZ=thetamaxZ/(nv-1)
for i=2:nv
    tmatrixX(i)=tmatrixX(i-1)+tstepX
    tmatrixY(i)=tmatrixY(i-1)+tstepY
    tmatrixZ(i)=tmatrixZ(i-1)+tstepZ
end
%Rotation about Y axis
for i=1:nv
    v=vmatrix(i,:);
    k=kmatrixY(i,:);
    theta=tmatrixY(i);
    v_rotY(i,:)=vector_rot(v,k,theta);
    % Mathworks FileShare Function
    % See function for details
end
%v_rotY=v_rot
%Rotation about Z axis
for i=1:nv
    v=v_rotY(i,:);
    k=kmatrixZ(i,:);
    theta=tmatrixZ(i);
    v_rotZ(i,:)=vector_rot(v,k,theta);

```



```
end
%Rotation about X axis
for i=1:nv
    v=v_rotZ(i,:);
    k=kmatrixX(i,:);
    theta=tmatrixX(i);
    v_rotX(i,:)=vector_rot(v,k,theta);
end
%v_rotX=v_rot
v_rotX
v_rotY
v_rotZ
%v_rotZ=v_rot
figure(1)
subplot(2,1,1), plot3(vmatrix(:,1), vmatrix(:,2), vmatrix(:,3)),
grid, xlabel('x'),ylabel('y'),zlabel('z')
subplot(2,1,2), plot3(v_rotZ(:,1),v_rotZ(:,2),v_rotZ(:,3)),
grid, xlabel('x'),ylabel('y'),zlabel('z')
%% Step Graph (each seperate rotation)
figure(2)

subplot(2,2,1), plot3(vmatrix(:,1), vmatrix(:,2), vmatrix(:,3),'.'),
grid, xlabel('x'),ylabel('y'),zlabel('z'),title('Original Tail')

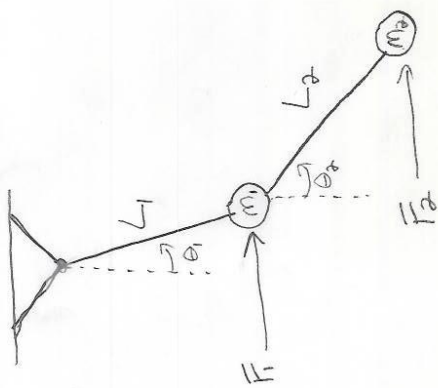
subplot(2,2,2), plot3(v_rotY(:,1),v_rotY(:,2),v_rotY(:,3)),
grid, xlabel('x'),ylabel('y'),zlabel('z'),title('Rotate about Y')

subplot(2,2,3), plot3(v_rotZ(:,1),v_rotZ(:,2),v_rotZ(:,3)),
grid, xlabel('x'),ylabel('y'),zlabel('z'),title('Rotate about Z')

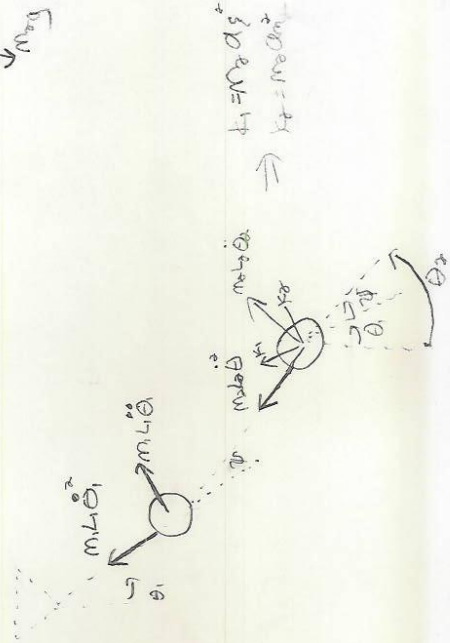
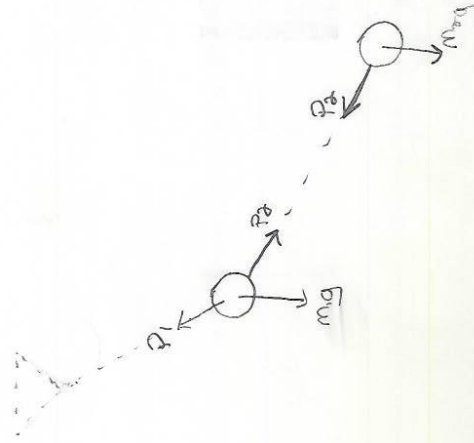
subplot(2,2,4), plot3(v_rotX(:,1),v_rotX(:,2),v_rotX(:,3)),
grid, xlabel('x'),ylabel('y'),zlabel('z'),title('Rotate about X')
```

**APPENDIX 2: DOUBLE PENDULUM MODELING**

Modeling Double Pendulum



Kinematic Diagram



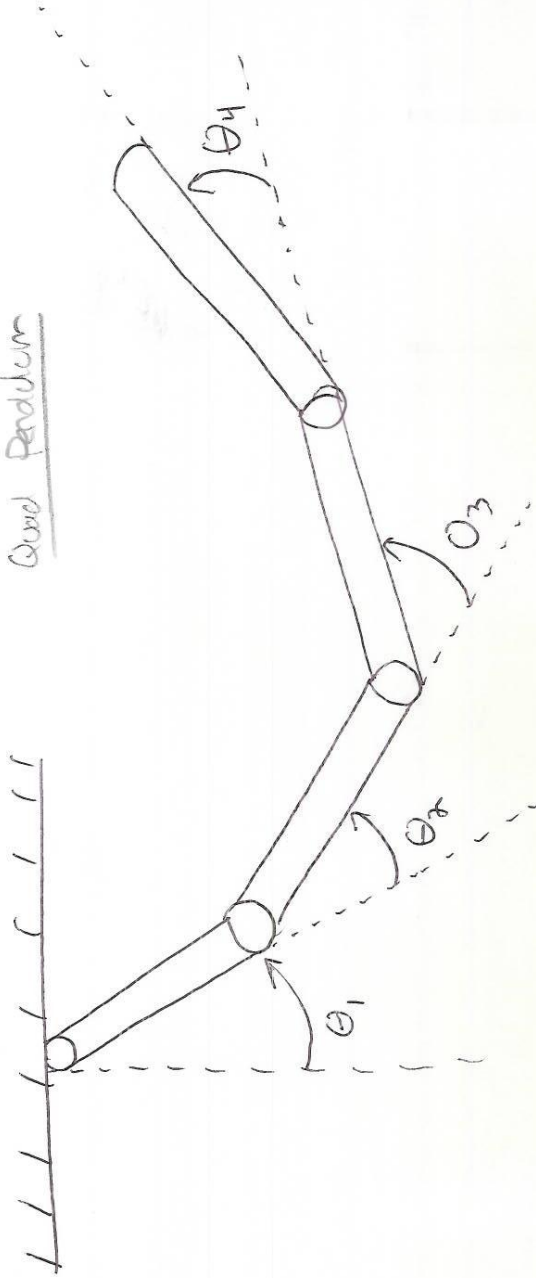
$$\begin{aligned} \dot{x}_1 &= L_1 \dot{\theta}_1 \\ \dot{x}_2 &= L_2 \dot{\theta}_2 \end{aligned} \Rightarrow$$

# APPENDIX 3: QUAD PENDULUM MODELING AND INERTIA CONTROL

Appendix Section 2

Moment of Inertia

Quad Pendulum



$$I(\theta)\ddot{\theta} + c(\theta, \dot{\theta})\dot{\theta} = \tau + \gamma + \delta$$

$I$  = moment of inertia matrix

$c$  = Coriolis effect matrix

$\tau$  = torque associated w/ external motors

$\gamma$  = gravity

$\delta$  = dissipation

$\theta$  = vector of relative link  $\phi$ s

$$I(\theta)\ddot{\theta} + c(\theta, \dot{\theta})\dot{\theta} = \tau + \gamma + \delta$$

For Planar

↳ ignore Coriolis effect term

↳ planar manipulator

↳  $\delta$ : angular velocity

↳ torque friction of motors ignored

↳ Assume all links in manipulator after a given pivot moves as a fixed body and all before are fixed.

↳ Diagonalization of Inertial Matrix

$$r_i = \begin{bmatrix} x_i \\ y_i \end{bmatrix} \quad \text{Location of } i\text{th pivot} \\ (r_i = [0, 0]^T)$$

$m_i, l_i$ :  $i$ th mass/length

$\theta_i$ : Angle between  $i$ th and  $(i-1)$ th link

Parallel Axis Theorem (Moment of Inertia)

$$I_n = \sum_{i=1}^n I_{e_i} + m_i \left| \frac{\vec{r}_i + \vec{r}_i}{\sigma} + \vec{r}_n \right|^2$$

$\sigma$ : center of mass

$$I_n = g \sum_{i=n}^n m_i \left| \frac{x_{i+1} + x_i}{\sigma} \right|^2$$

$$I_{0i} = m_i \frac{l_i^2}{12}$$